UNIVERSITY OF TURKU

Development of robust workflow for rescue of coxsackievirus A9 from cDNA clone

Institute of Biomedicine
MDP in Biomedical Sciences, Drug Discovery and Development
Master's Thesis

Author(s):
Sakari Vatunen

Supervisor(s):
Docent Petri Susi, Institute of Biomedicine, University of Turku

14.5.2025
Turku

Master's thesis

Subject: Institute of Biomedicine, MDP in Biomedical Sciences, Drug Discovery and Development
Author(s): Sakari Vatunen
Title: Development of robust workflow for rescue of coxsackievirus A9 from cDNA clone
Supervisor(s): Docent Petri Susi, Institute of Biomedicine, University of Turku
Number of pages: 61 pages
Date: 14.5.2025

Human picornaviruses cause mild flu-like illnesses and in some cases, heart or brain infections. Picornaviruses can be detected by specific and sensitive RT-qPCR and genetically typed by amplification of variable genome region for sequencing. However, full-length amplification of picornavirus genomes and virus rescue have not been optimized. Long PCR offers the possibility to amplify full picornaviral clones and to add a T7 promoter into the PCR products. These PCR products can be transfected into cells producing T7 RNA polymerase recognizing T7 promoter. Thus, *in vivo* transcription of PCR product into virus RNA occurs, which enables direct virus rescue. The virus rescue project with a plasmid cDNA clone of a human picornavirus, coxsackievirus A9 (CVA9), revealed at first that Platinum Super Fi II DNA polymerase had a sensitivity of 10^2 copies in amplification. The product specificity was good, and PCR reaction setup was also streamlined. Production of DNase-treated *in vitro* transcribed RNA from PCR products proved to be successful in conjunction with fluorometric quality control assays for RNA. In subsequent 2-step full-length RT-PCR experiments, Induro reverse transcriptase had a sensitivity of 10^5 copies with heterogenous CVA9 RNA samples. Finally, a CVA9 cDNA clone containing the enhanced green fluorescent protein (EGFP) reporter gene insert was used to generate PCR products with a T7 promoter by regulatory primers. T7-BSR cells expressing T7 RNA polymerase were used in virus rescue by transfecting CVA9-EGFP-T7 PCR products into them. EGFP signal indicating viral replication was successfully detected via fluorescence microscopy. However, transfection efficiency was suboptimal. In the end, virus rescue by T7-BSR cells is an efficient technique according to data obtained during the project, but full protocol needs further validation.

Key words: PCR, viral cloning, coxsackievirus A9, virus rescue, RNA polymerase

Table of contents

1 Introduction

Modelling of virus infections is often complicated due to lack of appropriate methods that would allow virus infection to be followed at high resolution. Current genetic methods are often unsuitable for rapid analysis of viral functions. In practice, this significantly impedes the development of the longed-for antiviral drugs and vaccines. *Picornaviridae* virus family, which includes a high number of significant human pathogens such as polioviruses and enterovirus A71, is a typical example of virus group against which we have very little countermeasures. There are practically no vaccines or drugs against human picornaviruses. In the field of drug development, the high number of different species and types impedes identification of potential drug targets, which is accompanied by the lack of high-capacity screening methods (Andino et al., 2023). Moreover, picornaviral RNA polymerase lacks proofreading capacity for which the mutation rate of picornaviruses is high. This leads to antigen diversity and poor cross-protection between different virus types. Thus, herd immunity against picornaviruses is not achieved, and the disease burden remains high because many picornavirus types are circulating at any given time.

Effective vaccine and drug development as well as pathogenesis studies on human picornaviruses necessitates the use of the genetically modified viral complementary DNA (cDNA) clones. A rescue method is also required to recover viruses *in vivo* from a cDNA clone transfected into cells. Robust long PCR protocols enable the rapid amplification of the viral genome for the transfection into the cells to establish the *in vivo* models (Lindberg et al., 1997). However, long PCR has not been fully applied to picornavirus research even though DNA polymerases capable of amplifying over 30 kbp targets have been available for years and polymerase formulations are evolving (Śpibida et al., 2017). This is significantly more efficient compared to the fragment-based viral clones, which are constructed by using multiple restriction enzymes and several intermediate steps. In addition, fragment-based cloning may not result in a functional cDNA clone and requires more studies to verify the functionality of the cDNA clone. Thus, more efficient methods for full-length amplification of picornaviral genomes are required to maintain genome integrity.

Mutagenesis of viral genome is central in studies of viral pathogenesis and lifecycle. Mutagenized enteroviruses have been previously used in determining the critical virulence factors of the picornaviruses (Al-Hello et al., 2009). In these experiments, the reporter gene is crucial because by following its expression virus infection can be detected rapidly and monitored intracellularly without disturbing cells. Heikkilä et al. (2011) demonstrated that existing viral cDNA clones can be edited by using mutagenic PCR primers in long PCR reaction to introduce accurate site-specific

mutations at high efficiency. This was followed by an efficient rescue protocol which enabled the entire rescue process to be streamlined. In this context, the interplay between PCR and cell culture experiments is considered crucial. Not only the PCR have to be able to amplify the cDNA clone for the transfections at high sensitivity and efficiency, but the PCR amplicons have to be produced in a form, which is readily suitable for virus rescue. In other words, the PCR product can be transcribed *in vivo* in living cells, which enables direct viral particle formation. Improved primer design with regulatory regions for transcription, robust reverse transcriptase (RT) and DNA polymerase enzymes and virus type-specific primer design should thus enable precise rescue of the viable viruses. This not only allows the virus functions to be analyzed with high throughput but also rational drug design in which precise information on picornavirus functions is required. Highly sensitive and simultaneously accurate RT-PCR will also have major implications for the healthcare system due to the improved capabilities for the rapid diagnosis of the picornavirus infections.

1.1 Classification of human picornaviruses

Viruses belonging to *Picornaviridae* family have been detected in both animals and humans. At present, 68 verified picornavirus genera are known with the involved 158 different recognized species. Of the 68 genera, the enteroviruses, rhinoviruses, and parechoviruses are considered the most relevant in the context of the infectious diseases in humans, while most of the genera are known to cause disease in animals only (Zell et al., 2021; Zell, 2018). Hepatoviruses, kobuviruses, and aichiviruses are other examples of the human picornaviruses but they do not have the same impact on the disease burden. The most important human picornaviruses belong to human entero- and parechovirus genera. Enteroviruses include polioviruses, coxsackieviruses, echoviruses and numbered enteroviruses. At present, rhinoviruses are also classified as a part of *Enterovirus* genus. *Picornaviridae* virus family is also characterized by a high mutation rate for which there are many different genetic types of picornaviruses. In the context of evolutionary relationships, the modern definition of the different picornavirus genera is based on the sequence homologies (Zell et al., 2021). According to this concept, human enteroviruses would have a distinct genetic profile compared to, for example, human parechoviruses, which enables effortless classification by sequence data. This fact is of great importance in virus research because PCR primer design or vaccine formulae is based on the genetic signatures of the conserved regions in the picornavirus genome.

1.2 Picornaviruses and human health

Although picornaviruses cause a wide range of infections among humans, the disease caused by any of the picornaviruses, such as rhinoviruses, is usually mild and uncomplicated, representing common cold spectrum of symptoms (Andino et al., 2023). It is estimated that over 50 % of all mild upper respiratory tract infections are caused by rhinoviruses, which means that picornaviruses afflict billions of people every year (Royston and Tapparel, 2016).

A typical example of an enterovirus-induced disease is the hand-foot-and-mouth disease (HFMD) that manifests itself in a combination of fever, blisters in the oral cavity, and varying types of rashes on the skin. The medically significant aspect of HFMD is the severity of the possible sequelae associated with it. Neurological complications caused by HFMD may include meningitis and even paralysis (Zhu et al., 2023). HFMD is often caused by enterovirus A species (coxsackieviruses A16, A10, A6 and enterovirus A71) of which coxsackievirus A16 and enterovirus A71 are the most strongly associated with HFMD (Aswathyraj et al., 2016). Enteroviruses have also caused concern to the healthcare system due to the neurological complications and viral infections of the heart muscle (Sin et al., 2015). Even though human picornavirus infections are generally mild, high number of cases and lack of drugs and vaccines in addition to risk of complications mean that the healthcare system faces problems in combatting against them (Royston and Tapparel, 2016).

Human rhinoviruses are the main cause of the common cold, which makes them one of the most significant epidemic factors throughout the world. Indirect expenses caused by rhinovirus-associated flu, including absences from work and complicated illnesses in, for example, immunosuppressive patients demonstrate the need for effective antiviral strategies. In general, rhinovirus infection cannot effectively spread around the body from respiratory epithelium because rhinovirus replication is the most optimal at approximately +33 °C (Royston and Tapparel, 2016). Some dangerous pathogens can induce massive cell death (necrosis) on respiratory epithelium, but rhinoviruses only affect cellular tight junctions in the respiratory epithelium, which may explain the low severity of rhinovirus infection. However, the leaky epithelium phenomenon may promote entry of bacteria into the lung tissue, which increases risk of bacterial pneumonia. In comparison to coxsackieviruses, rhinoviruses have limited tropism in terms of suitable host tissues and cells. Coxsackieviruses cause generalized infection in some cases because they can replicate at +37 °C and cross biological barriers of human body through unique mechanisms (Zhu et al., 2023; Sin et al., 2015). In summary, due to high tropism, coxsackieviruses can induce permanent and highly disabling complications, which do not apply to rhinoviruses.

1.3 Picornavirus genome and particle structure

The picornaviral genome is a linear, uncoiled positive-polarity RNA genome consisting of a single strand. The estimated length of the picornavirus genome is 7–9 kb. The 5’ ends of the picornavirus genome contain an internal ribosomal entry site (IRES) (Figure 1), which enables ribosome binding and initiation of translation (Lin et al., 2009).

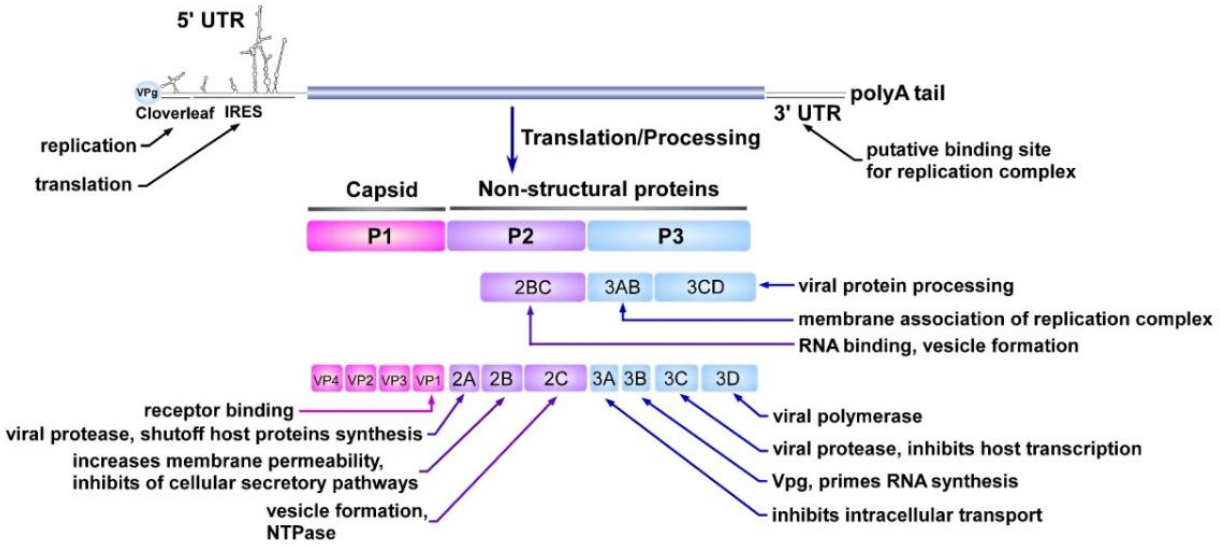

Figure 1. The general structure of the enterovirus genome as an example. The polyprotein P1 is cleaved into the structural proteins VP1–VP4 which are the crucial structural components of the viral capsid. The polyproteins P2 and P3 are cleaved into the non-structural proteins that affect, for example, the passage of the virus through the cell membranes. UTR, untranslated region. IRES, an internal ribosomal entry site. All picornaviruses share the single open reading frame and the polyproteins P1–P3. Obtained and modified from (Lin et al., 2009) under the terms of Creative Commons Attribution 2.0 License. https://creativecommons.org/licenses/by/2.0/.

The 5’ UTR of the picornaviruses is uncapped and can be over 1 000 bases in length. Thus, the initiation of the translation warrants the binding of the 40S ribosomal subunit directly into the IRES (Figure 1). However, the cellular microenvironment affects greatly translation efficiency because many nucleotide-binding proteins can interact with virus RNA (vRNA), which may explain the observed differences in cell susceptibility to the picornavirus infections (Bedard and Semler, 2004).

Picornaviruses can be classified as having self-cleavage capacity because the viral genome itself codes for the proteases and polymerase needed for genome replication and viral polyprotein processing, which enable production of functional viral proteins. The composition of the picornavirus genome (Figure 1) has a major effect on the mutation rate and the host-virus interactions. The viral 3D RNA-dependent polymerase has a high error rate, close to 10^{-3} according to some reports (Kok and McMinn, 2009), which explains the observed mutation rate among picornaviruses. This increases virus tropism and allows the virus to survive in challenging

environments. In the context of virology, quasispecies refers to the pool of the viruses generated by error-prone viral 3D RNA-dependent polymerase (Domingo et al., 2005).

Picornaviruses are non-enveloped, which means the virion is not enclosed by a membrane. The picornavirus capsid has a diameter of approximately 30 nm. The main structure of the capsid consists of 12 pentamer units that are formed when triangular protomers are unified into a pentamer (Figure 2) (van der Linden et al., 2015).

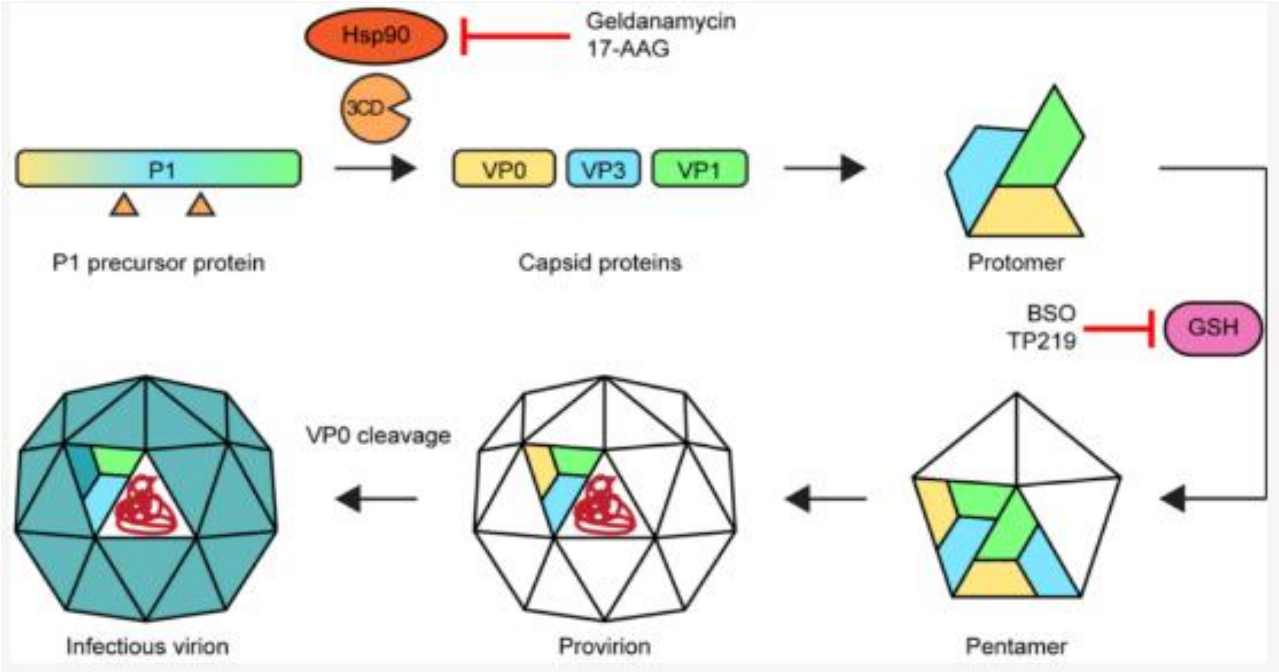

Figure 2. The enterovirus capsid assembly and the capsid structure. The viral structural proteins VP1, VP3, and VP0 from the polyprotein P1 precursor form the triangle-like protomer, which is a part of a pentamer unit. Cleavage into the capsid proteins is promoted by the viral protease 3CD and chaperone Hsp90. The final infectious virion consists of 12 pentamers, and the provirion becomes a mature virus particle when the protein VP0 is cleaved into the structural proteins VP2 and VP4. Glutathione (GSH) and Hsp90 are critical intermediate factors in the assembly for which they are proposed drug targets for antivirals (red lines pointing to Hsp90 and GSH). The figure was obtained, reproduced and modified from van der Linden et al. (2015) according to the terms of Creative Commons Attribution 4.0 license.
http://creativecommons.org/licenses/by/4.0/

Picornavirus capsid proteins are among the most characterized hypothetical drug targets of the antiviral drugs against picornavirus infections. Drugs can induce conformational changes in the capsid proteins which prevents the receptor-virus interaction crucial for virus entry. Picornavirus proteases are also identified as drug targets because some alkylating agents can induce irreversible loss of function of these proteases (De Palma et al., 2008).

1.4 Picornavirus replication cycle and cell-cell transmission

Picornavirus entry into the cells of the host organism is mediated through several receptors including low-density lipoprotein receptors, integrin receptors and coxsackie-adenovirus-specific receptor (Andino et al., 1999; Garmaroudi et al., 2015). According to this concept, different picornavirus species have varying affinities for different receptors, which determines viral tropism. Fusion of receptor-virus complex initiates endocytotic cascade, which ultimately leads to release of viral material inside a low pH endosome in the cytoplasm (Vázquez-Calvo et al., 2012). Genetic alterations in critical amino acid residues can affect 3D interactions between viral capsid proteins and human cellular receptors, which alters the binding efficiency and creates new possibilities of interaction.

Picornavirus entry into host cells can also be categorized by the shift of the structural status of the host cell membrane – endocytotic routes. When holes or other 3D adaptations in the cell membrane are formed, these changes are associated with specific protein families – clathrin-like or caveolae-like. For example, integrin-mediated endocytosis pathway is associated with clathrin activity whereas cholesterol receptor is associated with either dynamin activity or not, but not clathrin or caveolae protein families (Vázquez-Calvo et al., 2012).

There are also other major proteins that affect internalization and release of viral material inside the infected cells. The coxsackie-adenovirus-specific receptor is coupled with the decay accelerating factor enhancing the internalization, which is an important mechanism in coxsackievirus B infections (Garmaroudi et al., 2015). Among enteroviruses, infection pathways of CVA9 are unique. In case of CVA9, the infection cycle begins with alterations in the cellular actin cytoskeleton and formation of hole-like grooves on the host cell membrane after integrin-mediated binding of CVA9 to cell membrane. Initial viral entry of CVA9 to host cell is regulated by phospholipase C after which proteins belonging to endosomal sorting complex required for transport family are responsible for formation of large uniquely neutral multivesicular bodies from small endosomal vesicles. By *in vitro* binding assays it has been shown that Rac1 protein activity somehow affects final release of CVA9 vRNA genome to the cytoplasm where IRES elements of vRNA interact with host ribosomes. It has also been shown that αV integrin receptor family is responsible for binding of CVA9 to cell membrane but not internalization whereas *β2* microglobulin, dynamin and Arf6 proteins are necessary for cell membrane permeability changes observed during CVA9 infection and actual viral internalization. It remains unknown whether specific drugs targeting those beforementioned protein components of the infection pathway can,

for example, cause degradation of endosomes or disrupt crucial membrane-virus interactions of CVA9 (Andino et al., 1999; Huttunen et al., 2014).

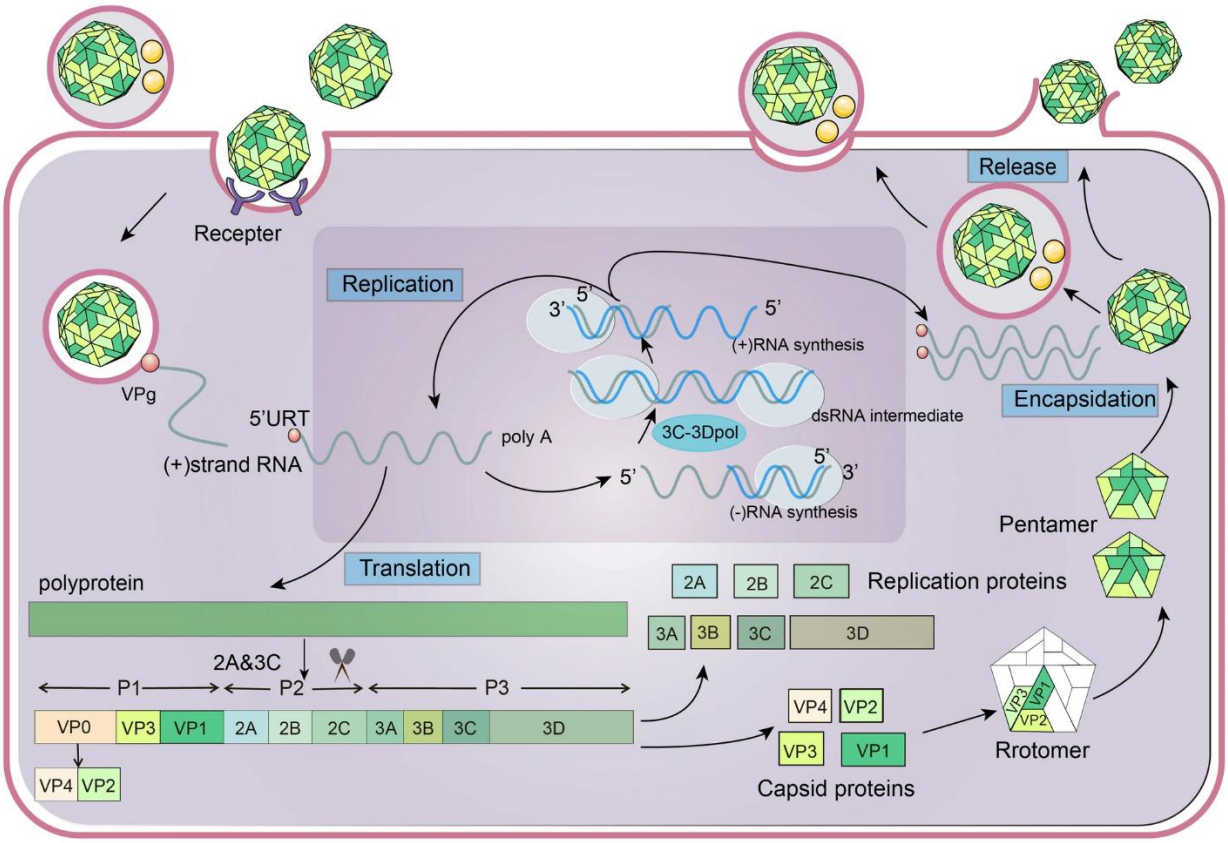

.

Figure 3. Summary of enterovirus lifecycle. After binding to receptor (e.g. integrin), the enterovirus is internalized via endocytosis, and the viral RNA is released inside the cell from late endosomes. Viral protein VPg acts as a stabilizer of released RNA so that translation via IRES elements can occur. Cleavage sites between junctions VP1/2A and 2C/3A enable the cleavage of the polyprotein into multiple viable virus proteins. Proteases also degrade host proteins during viral infection. Protomer of viral capsid is assembled from proteins VP1–VP4 whereas other proteins facilitate genetic replication. Viral release from host cells occurs via exocytosis or inside cellular vesicles containing degraded host material. This figure was obtained and modified from (Zhu et al., 2023) according to the terms and conditions of Creative Commons Attribution 4.0 International License. https://creativecommons.org/licenses/by/4.0/

Picornaviruses utilize a unique translation pattern independent of the host organism, which surrounds the pathogenicity and lifecycle of picornaviruses (Figure 3). Cellular translation in the host is based on capped mRNAs, but picornavirus proteases inhibit cap-binding proteins which in turn prevents translation of host mRNAs – a possible mechanism behind cell death during viral infection (Belsham, 2009).

Besides cellular receptors, it has been shown that picornaviruses can spread independent of receptors. Figure 4 below describes the complex nature of human coxsackievirus infections and receptor-independent spread of infection. LC3II is a protein associated with the autophagy pathway. The autophagy compiled with the extracellular microvesicles enables the virus to hide and move

inside those microvesicles outside the reach of the immune system, which increases tropism (Sin et al., 2015). Thus, antiviral drugs against picornaviruses may be hard to develop by blocking viral receptors and because autophagy pathways are highly diverse compared to simple virus receptors druggable by traditional compounds. Autophagy inhibition would be effective against the serious complications including infections in the brain because autophagy is necessary for penetration of blood-brain barrier.

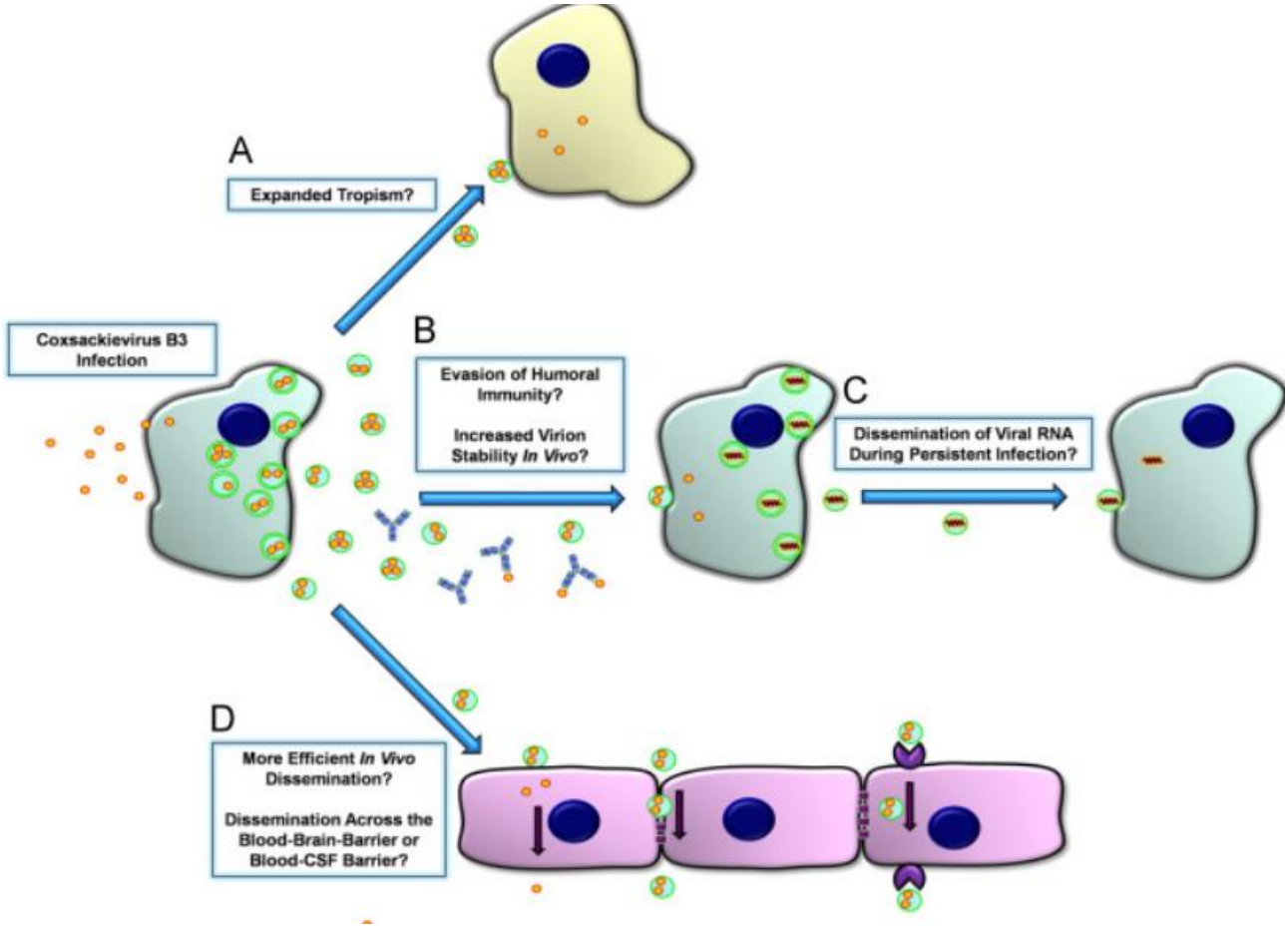

"Figure [4]. Model of CVB dissemination in the host by shed EMVs. High numbers of LC3II+ extracellular microvesicles (EMVs) containing infectious virus were recently observed following infection of progenitor cells in culture. Both the differentiation process and viral infection may enhance shedding of single membrane EMVs derived from the autophagy pathway. (A) Virus-associated EMVs may expand the natural tropism of CV to target cells which fail to express canonical virus receptors. (B) Neutralizing antibodies may be ineffective against infectious virus sequestered within the protected environment of the extracellular microvesicle. Also, virus-associated EMVs may increase the stability of infectious virus within the host during hematogenous spread. (C) EMVs may assist in viral RNA dissemination during the persistent stage of infection whereby the presence of intact virions and/or structural viral proteins may be limited. (D) EMVs may help virions travel and enter new target tissues and cross selectively permeable barriers." This figure and its caption text have been reprinted in full from *Virology*, volume 484, Jon Sin, Vrushali Mangale, Wdee Thienphrapa, Roberta A. Gottlieb, Ralph Feuer, Recent progress in understanding coxsackievirus replication, dissemination, and pathogenesis, Pages 288–304, Copyright (2015), with permission from Elsevier.

The ability of some picornaviruses including coxsackieviruses to cause severe complications may be related to their ability to enter the cells via complicated pathways that bypass the restrictions based on normal cellular receptor expression or epithelial barriers (Figure 4).

To enlighten the immunological factors surrounding viral replication, picornaviruses can evade the human immune system by inhibiting the pathways associated with, for example, the production of the interferons necessary for the immune system to combat against the virus infections (Zhang et al., 2020). Partly due to this, the elimination of the picornavirus infections is complicated and the viral evolution leads to seasonal epidemics characterized by new variants that cause altered immune response by mutated viral proteins interacting with interferon pathways. This is comparable to the characteristics of, for example, the influenza viruses (Zhang et al., 2020; McCullers, 2016).

1.5 Long PCR and associated issues in virus research

Long PCR refers to a specific form of PCR protocols that aim to amplify long genomic fragments in a single step. In practice, most standard PCR protocols are designed for gene amplification at range of 300–3 000 bp whereas quantitative PCR (qPCR) amplifies short fragments less than 300 bp in length. In contrast to this, virus research necessitates the amplification of the full viral genomes, which range 2 600–150 000 bp in length. Many virus genomes possess multiple critical structural elements which makes the production of the clones of those genomes complicated. During long PCR, it is essential that the rate of the errors or mismatches is low because otherwise the integrity of the nucleotide sequence is compromised during amplification, which affects virus replication and production of viable virus particles. If the virus genome is amplified so that multiple primer pairs yielding multiple fragments are used, the process becomes slow and susceptible to errors. According to various reports, the factors guaranteeing the high-performance amplification of the picornavirus genomes are partly unoptimized due to the undersized resourcing of the long PCR research (Lazouskaya et al., 2014).

The stability and reproducibility of the long PCR protocols is a growing issue when long PCR is become more adapted into various operations in virus research. This issue has major implications for the use and development of DNA polymerases. Because virus genomes can be long (up to 150 kbp), the error rate becomes an invaluable factor. Some DNA polymerases may demonstrate error rates below 10^{-6} but this is accompanied by other complex experimental success factors like special PCR cycling undermining the feasibility of the use of those enzymes (Lazouskaya et al., 2014).

An effective DNA polymerase enzyme has proofreading capacity, which means that it can correct the mistakes during amplicon elongation in PCR. However, PCR primer degradation is detected if the 3' to 5' exonuclease activity is too high (Terpe, 2013). This may prevent amplifying viral clones for sensitive purposes like vaccine development or diagnostics. Recombinant DNA polymerases can be genetically engineered with various gene editing techniques to eliminate the degradation problem but the length of the DNA to be amplified remains a plausible permanent issue and causes limitations. According to experimental data, genetic modifications have rarely desired effects on the template length limit of the enzyme (Nishioka et al., 2001).

1.6 Picornaviral cloning and viral rescue via combination of PCR protocols

Successful virus rescue refers to the ability to produce fully viable viruses by using the PCR-amplified viral cDNA clones as templates for *in vitro* or *in vivo* transcription in which infectious vRNA is produced and from which virus particles form after genome replication. In the context of picornaviruses, the genome is both long (approximately 7 kb) and compact with highly specialized regulatory elements for which the editing of the genome without compromising the integrity of the virus functions is complicated (Ji et al., 2023).

Even though long PCR for picornaviruses has been applied to practice since the 1990s, the production of good quality clones without introducing mutations to the genome is still a highly evolving subject. Traditional long PCR methods for picornaviruses include the use of multiple DNA polymerases as a mixture to overcome the limitations associated with the low proofreading activity of the traditional bacterial *Thermus aquaticus* (*Taq*) polymerases (Leister and Thompson, 1996). In addition, fragment-based PCR was often used to assemble full genome, and single fragments representing the picornavirus protein coding genes and the non-coding termini (5' or 3' ends) often had low coverage and chances for mutations. Such strategy often complicated primer design and binding (Hymas et al., 2008). However, modern long PCR enzymes with both high fidelity and ability to amplify long fragments have largely replaced traditional methods. Thus, high fidelity and amplification range are the most important and critical factors for the success of long PCR. In addition, long PCR enzymes should have high sensitivity since virus amount in clinical samples is often low, which poses a challenge for genome amplification by DNA polymerase. By using long PCR, it is possible to include new regions to genomic termini, which may make virus replication more effective.

1.7 Background of this study

Historically, virus rescue from viral cDNA clones has been conducted by using *in vitro* transcription (IVT) in which cDNA (viral genome cloned into a plasmid under T7 promoter) acts as template in IVT reaction to produce vRNA, which is transfected into cells for virus replication. Such method is rather complicated, contains many steps, and is sensitive to contamination. Previously, it has been shown that PCR-based methods can be used to add specific promoter sequences to the 5' end of PCR amplicon, which will direct the expression of the gene or genome cloned behind the primer region. T7 promoter is recognized by T7 RNA polymerase (T7RNAP), which was originally discovered while studying bacteriophages, and it is well characterized (Borkotoky and Murali, 2018). It is a valuable tool in research because mammalian cells support cytoplasmic production of viable T7RNAP directly from an inserted transgene coding for T7RNAP (Dunn et al., 1988). T7RNAP recognizes specific and short T7 promoter, which acts as initiator of T7RNAP-driven transcription of DNA into RNA. The specificity of T7RNAP for T7 promoters is high which is helpful in precise regulation of gene expression (Sandig et al., 1993).

Combination of T7 promoter and T7RNAP can be used in gene expression studies. A gene coding for T7RNAP can be transfected into cells that do not intrinsically express T7RNAP gene by virtue of different plasmids. It can drive the expression of any genetic element transfected into these cells. While these elements containing T7 promoter are readily transcribed within cells, it has been shown that a dual promoter composition is the best since it enables autoregulation of T7RNAP gene expression (Brisson et al., 1999). This can be achieved via ligating cytomegalovirus (CMV) promoter and T7 promoter in front of a gene encoding T7RNAP (i.e. CMV-T7-T7RNAP). The CMV promoter can be read by human RNA polymerases, and it is thus functional in most native human cells. Once T7RNAP cloned under CMV is expressed, the produced T7RNAP can bind to the T7 promoter in the gene construct and drive expression of T7RNAP. This significantly enhances the production of T7RNAP mRNA with over 50-fold improvement and with no significant cytotoxic effects (Brisson et al., 1999).

In practice, T7 promoter readable by T7RNAP can be added to 5' ends of PCR products produced from viral cDNA clones via PCR primers designed for this purpose. Cells that directly express T7RNAP can be constructed with modern techniques which enables genuine *in vivo* transcription of viral cDNA into replicative and infectious vRNA with higher efficiency than by using basic plasmids coding for T7RNAP (Fu et al., 2021). These direct cell-based methods also avoid the

transfection step of the T7RNAP-coding plasmids, which consumes time and has limited performance.

Although recombinant T7RNAP-expressing cell lines have been generated, their susceptibility to picornavirus types remains unknown because only a few types have been tested with these cell lines (Zheng et al., 2009). It also remains poorly understood how to transfect the viral cDNA into the cells for *in vivo* transcription to obtain both the best transfection and transcription efficiency – either as a plasmid cDNA or a PCR amplicon. Because the precise modification of the picornavirus genome is a complex procedure, high-end PCR and genetic engineering methodologies are required. In unsuccessful attempts, the long PCR produces mutations that render the viral genome not capable of replicating in the cells. The insertion of the recognized reporter gene constructs including EGFP (Heikkilä et al., 2011) or other foreign peptide sequences may interfere with normal polyprotein cleaving or capsid assembly. Recent advantages suggest that inserting foreign peptides as a part of the picornavirus capsid structure is possible by modern genetic engineering and proteomics-based methods (Lyu et al., 2015).

In summary, the reliability of long PCR is instrumental to the infection experiments involving picornaviruses. Mutations during cDNA amplification may render the viral clone incapable to replicate in the cells or lead to altered results if the crucial amino acids for viral replication are mutated randomly. Sometimes long PCR may generate products that are of weak quality which impedes the experiments. Thus, the reduction of the intermediate steps and using carefully optimized reporter gene constructs is essential in using cDNA clones as the source of the viral genetic material that can infect cells in experiments focused on studying viral lifecycle (Heikkilä et al., 2011). Modifying cDNA clones through genomic insertions can be complicated but accurate strategies reduce the risk of the errors. For example, miRNA and transposase proteins from bacteriophages can be utilized in modifying viral clones in the relevant fields of vaccine research or genetic engineering (Vilen et al., 2003; Liu and Luo, 2021).

1.8 Key hypothesis and objectives of this project

This project is based on the clone of the coxsackievirus A9 (CVA9), which belongs to the human enterovirus B species of the genus *Enterovirus* according to modern taxonomy of enteroviruses (Steil and Barton, 2009; Zell, 2018).

First, it is hypothesized that long PCR can be efficiently used in amplifying viral cDNA clones including plasmid clone pCVA9 and modifying these clones. One of the main objectives of this

project was to utilize special PCR primer sets with T7 promoter, and other special primers to add genomic regulatory elements to the PCR products. It is proposed that the special PCR primers can improve the replication of the PCR-amplified viral clone in the cells into which the clone is transfected. In the context of the long PCR, the project aimed at improving the sensitivity of the long PCR by establishing methods for optimizing crucial PCR parameters and finding the best enzymes and reagents for amplification of CVA9 cDNA clone from a plasmid template.

Secondly, it is hypothesized that the effective long PCR can be combined with highly efficient RT enzyme to make a generalized protocol for amplifying any type of, for example, coxsackievirus RNA genome as cDNA obtained in the RT step. This project aimed at streamlining the workflow for obtaining and amplifying the cDNA clones because the high number of intermediate steps could generate mutations in the clones so that the clones would not be able to replicate in the experimental cell lines.

It is proposed that by using CVA9-EGFP clone containing the enhanced green fluorescent protein (EGFP) reporter construct, T7RNAP-producing cell line T7-BSR, and T7RNAP-coding plasmids in cell experiments, the workflow for virus rescue and monitoring of virus infection could be simplified. In context of T7RNAP, this project aimed at characterizing T7RNAP-coding plasmids containing a T7-CMV dual promoter composition to improve T7RNAP expression in human cells into which T7RNAP-coding plasmid must be transfected. Overall, it is hypothesized that the combination of regulatory primers in long PCR, successful transfection and EGFP reporter enable robust rescue of CVA9 virus from cDNA clone. In essence, verification of T7RNAP-producing T7-BSR cell line as a suitable host for EGFP-bearing picornavirus clones would have a major impact on picornavirus research along the T7 promoter hypothesis.

1.9 Experimental design

The first objective of this study was the development of a robust workflow for amplification of CVA9 and CVA9-EGFP plasmid clones by virtue of long PCR with high-fidelity DNA polymerases. Each of the tested DNA polymerases was subjected to copy number sensitivity testing. In practice, dilution series of each plasmid was prepared so that final copy number controls were generated by using validated prior-constructed stock plasmids. The generated dilution series were verified by using reverse-transcription quantitative PCR (RT-qPCR) to demonstrate that the cycle of quantification (C_q) values and their differences in RT-qPCR match the expected values based on the 10-log composition of the full dilution series. An independent copy number standard was also included in the qPCR assays. The stock plasmids of CVA9, CVA9-EGFP and a few

T7RNAP-coding plasmids were sent to be sequenced by a specialized commercial service provider (Eurofins Ltd., Germany) to verify the composition of the plasmids including regulatory elements of the CVA9 genome.

The PCR enzyme with the best copy number sensitivity in terms of CVA9 and CVA9-EGFP cDNA amplification was selected as the DNA polymerase to be used during RT-PCR protocol. The testing of the RT enzymes was another major aim of this study because validated RT-PCR has several advantages in cell-based infection experiments. RT-PCR can be used to test the infected cells, which verifies replication of vRNA in the infected cells. Inoculation of viral particles from the infected primary cells to non-infected secondary cells was also included in the experimental plan to demonstrate that the viruses rescued from cDNA clone were mature virus particles capable of inducing a secondary infection.

The transfection was based on either *in vitro* transcribed vRNA, extracted vRNA, plasmid containing CVA9-EGFP cDNA or PCR products obtained by using the plasmid CVA9-EGFP as template for long PCR involving standard and regulatory primers. Transgenic T7-BSR cells producing T7RNAP were used in the transfection step whereas human lung cancer cell line A549 was used in the secondary infections and as a control because A549 cells express integrin receptors necessary for enterovirus-induced infection (Heikkilä et al., 2010). After the transfections, the stepwise monitoring of the infected cells by detecting EGFP fluorescence and by applying immunofluorescence assays to fixed cells enabled the evaluation of the differences in virus loads in relation to what was transfected.

2 Results

2.1 Plasmids and copy number sensitivity tests

2.1.1 Evaluation of plasmid integrity

To begin with, plasmids used in the study were analyzed on agarose gels. Copy number sensitivity results were obtained by agarose gel runs of full 20 µl PCR reactions representing different copy numbers of the plasmid containing CVA9 cDNA labelled as clone pCVA9-1 as the template of PCR. The number of plasmid copies in the 1 µl PCR sample added to the final 20 µl reaction was used as the determination of the sample copy number. The 1 µl PCR sample was obtained from stocks of 10-fold dilution series in the range from 10^7 to 10^0 copies/µl, which were verified by qPCR with copy number standards (data not shown). If the photograph obtained by UV imaging of the gel showed a clearly visible specific band, it was considered as a positive result in context of copy number sensitivity or integrity check. It was observed that the agarose gel system was robust with no evidence of degraded molecular weight ladders, aberrant migration of DNA or enlarged bands.

The plasmid pCVA9-1 was also analyzed by gel electrophoresis in conjunction with the other three CVA9 plasmids, namely pCVA9-EGFP-6, pCVA9-EGFP-7, and pCVA9-EGFP-11. All plasmids demonstrated high integrity while amplified by long PCR and the repeatability of the process was considered optimal. Extensive spectrophotometric measurements and qPCR analysis against standards indicated that all of the plasmids were intact and free of possible highly contaminating substances including solvents (data not shown). To conclude, the plasmid clone labelled pCVA9-1 was used to test the collection of long PCR enzymes on a large scale.

2.1.2 Long PCR performance with different kits

In total, 6 different long PCR kits were tested. Of the 6 tested kits, 2 robust kits (Platinum Super Fi II and repliQa HiFi Tough Mix) provided sufficient yields of specific products, and they were consistent in their performance when tested with the standard protocols in section 4.2. Even though the number of used cycles was as high as 40, Platinum Super Fi II still managed to amplify the desired target with a minimal number of non-specific products (Figure 5 on the next page). Further results also confirmed that the performance of Platinum Super Fi II did not depend on the characteristics of the input material. There were also no signs of unexplained poor performance. This was considered as evidence of robustness required in producing PCR products for sequencing,

transfection or IVT-RNA production. Overall, the copy number sensitivity of Platinum Super Fi II in amplification of pCVA9-1 was very good because only 10^2 copies produced a positive result on agarose gel (Figure 5A).

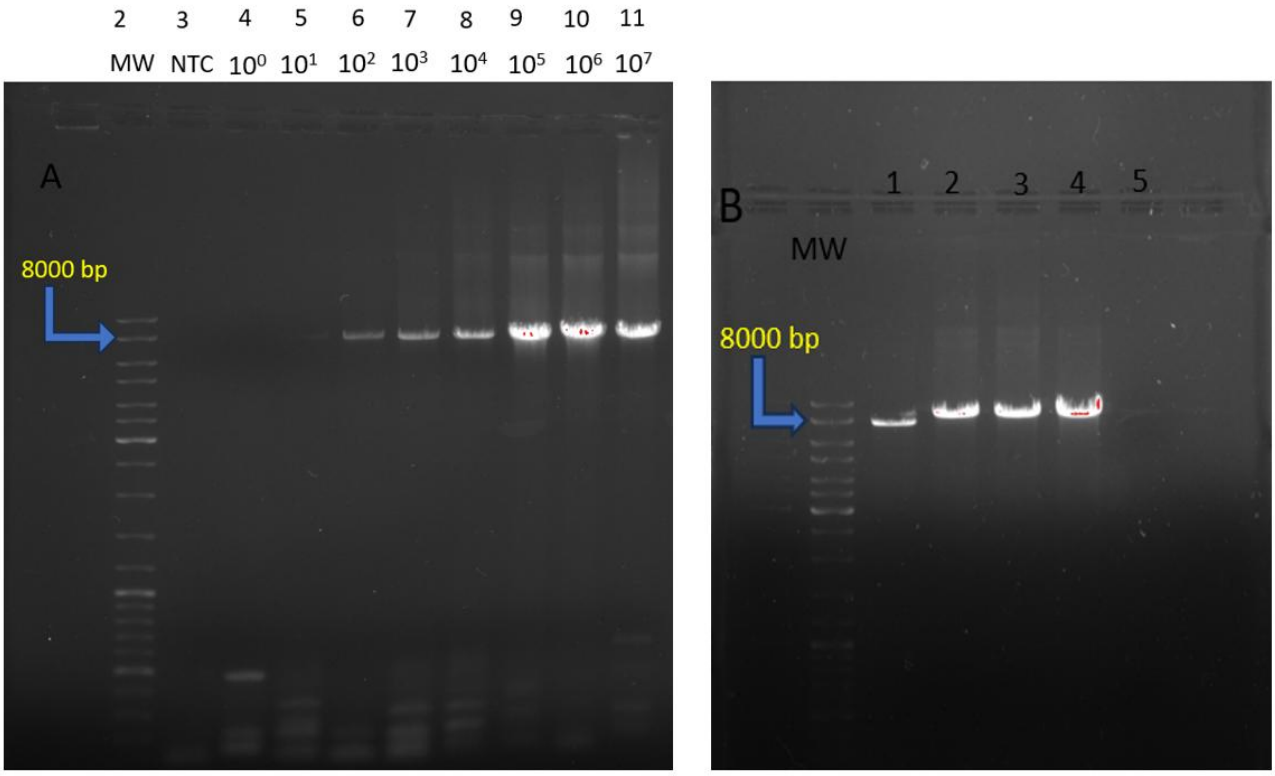

Figure 5. Agarose gel electrophoresis of pCVA9-1 PCR products obtained by Platinum Super Fi II enzyme (40 cycles). (A) pCVA9-1 dilutions 10^7–10^0 copies/µl as PCR samples, lanes representing PCR product mixes and controls marked by sample copy number and sample ID from left to right (lanes 2–11). (B) Constant sample copy number 10^6 copies/µl, lanes numbered by template cDNA clone used in PCR: 1 = pCVA9-1, 2 = pCVA9-EGFP-6, 3 = pCVA9-EGFP-7, and 4 = pCVA9-EGFP-11, 5 = NTC. NTC, no template control, MW, molecular weight ladder Gene Ruler Mix 100–10 000 bp with 8 000 bp band separately marked. Red color in the image, saturated pixels. Gel, 0.8 % agarose. Full 20 µl PCR reactions were loaded on the gel as samples, respectively.

The sensitivity of Prime Star GXL was considered weak because only sample copy numbers 10^7 and 10^6 produced any bands in the gel electrophoresis. CVA9-PCR products obtained by Q5 and Phusion HotStart II only produced a band representing sample copy number 10^7 in addition to which KAPA Hifi PCR products did not produce any band. Thus, of the tested enzymes, results obtained by virtue of KAPA Hifi, Q5, Phusion, and Prime Star GXL are not disclosed here. On the basis of Figures 5A and 5B, it can be stated that the prior-constructed stock plasmids pCVA9-1, pCVA9-EGFP-6, pCVA9-EGFP-7, and pCVA9-EGFP-11 were viable. The size of the genomic cDNA of CVA9 is approximately 7 500 bp without any insert and 8 200 bp with the EGFP reporter gene insert. The bands produced when repliQa HiFi Though Mix was used as the PCR kit in long PCR amplification of pCVA9-1 are shown in Figure 6.

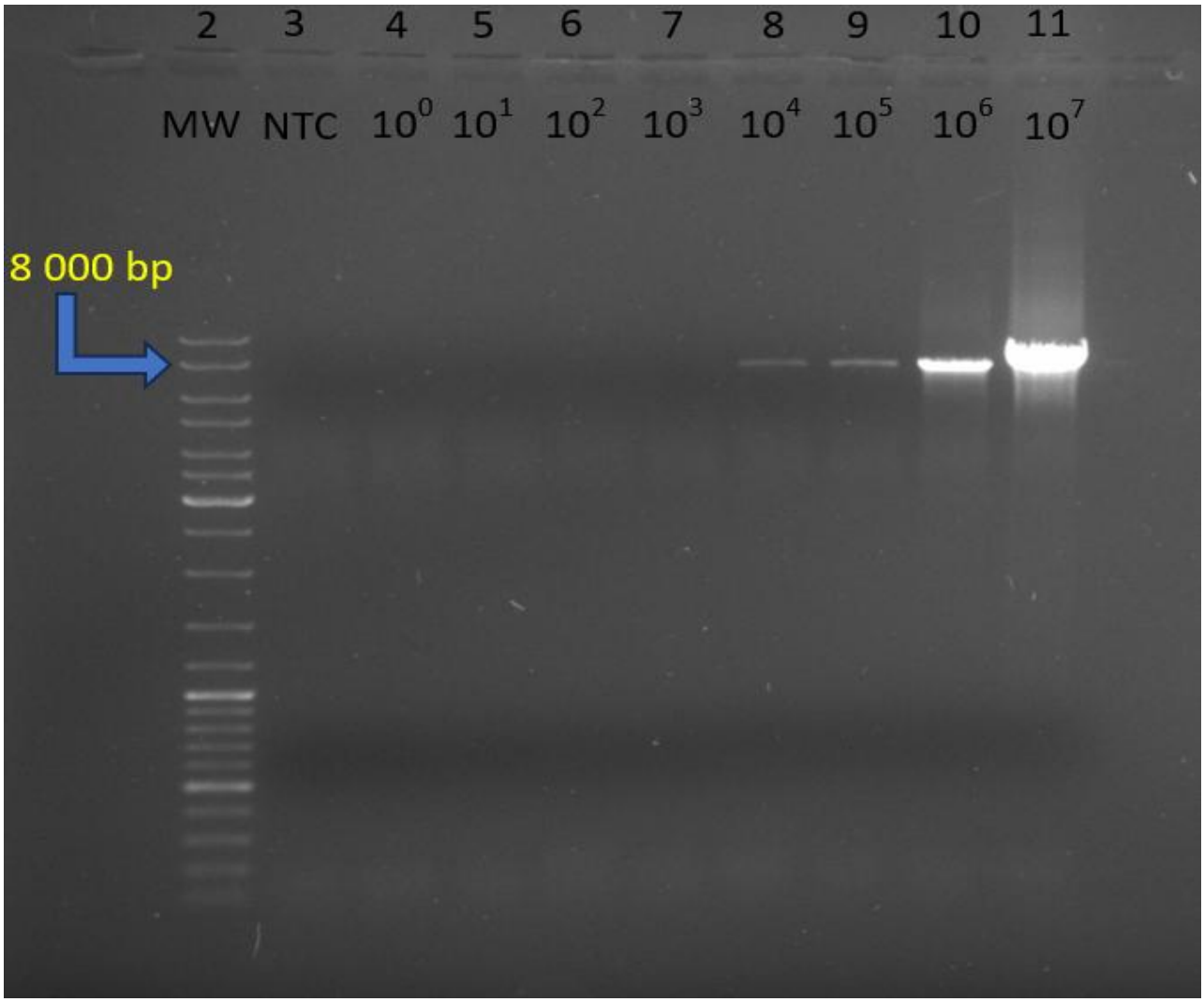

Figure 6. The gel image of the agarose gel electrophoresis of pCVA9-1 PCR products obtained by repliQa HiFi Tough Mix PCR kit with 35 cycles. Wells on lanes 2–11 were loaded with molecular weight marker, control reaction and full 20 µl PCR reaction product mixes, respectively. MW, molecular weight ladder Gene Ruler Mix 100–10 000 bp and 8 000 bp band separately highlighted. NTC, no template control with water. Exponent label 10^x indicates the copy number of pCVA9-1 in the 1 µl sample loaded into the PCR reaction. Gel, 0.8 % agarose.

According to Figure 6, the sensitivity of repliQa HiFi Though Mix was 10^4 copies/µl when pCVA9-1 cDNA was the template, which can be considered as good sensitivity when the approximate length of the product, 7 500 bp, is considered. Based on Figure 6, it can also be evaluated that repliQa Hifi Tough Mix Kit succeeded in the production of the specific PCR amplicons because no smearing or degraded amplicons can be observed.

2.2 RT-PCR and quality of RNA samples

2.2.1 Optimization of RT-PCR performance

CVA9 RNA samples and cDNAs were first analyzed via RT-qPCR to determine the integrity of the prepared RNA dilution series on a small scale. Some produced cDNAs and enzymes demonstrated

poor quality according to RT-qPCR for which certain samples and RT protocols were excluded to find the optimal protocol. During the initial testing of the RT enzymes and protocols, CVA9-EGFP-IVT RNA was not viable, and no results were obtained because of residual DNA contamination probably disrupting the annealing of the CVA9-R gene-specific primer used in the testing. After this, oligo-dT primer system demonstrated better integrity of cDNA products. This was indicated by amplification efficiency in RT-qPCR according to further testing into which acceptable range of amplification efficiency [0.90; 1.10] was applied (data not shown). In addition, LunaScript was not used in further testing because the performance of Induro RT, for example, was significantly better with long targets than that of LunaScript.

Greater yield of full-length cDNAs were obtained by using oligo-dT primers than gene-specific primers in full-length RT-PCR of CVA9. This was considered important due to the variable quality of some samples, which posed a challenge to full-length cDNA synthesis.

Oligo-dT-synthesized cDNAs were used as long PCR templates in 2-phase RT-PCR so that Platinum Super Fi II protocol was used for PCR amplification step (see section 4.2). In Figures 7A and 7B are presented the sensitivity of qScript Ultra Flex kit and SuperScript IV in full-length cDNA synthesis by using CVA9 RNA extracted from purified viruses as the template. The sensitivity of qScript is limited to $2 \cdot 10^7$ RNA copies only whereas SuperScript IV appears to have a sensitivity cutoff of $2 \cdot 10^6$ RNA copies, but more non-specific bands are seen on the agarose gel (Figure 7B) than in case of qScript (Figure 7A).

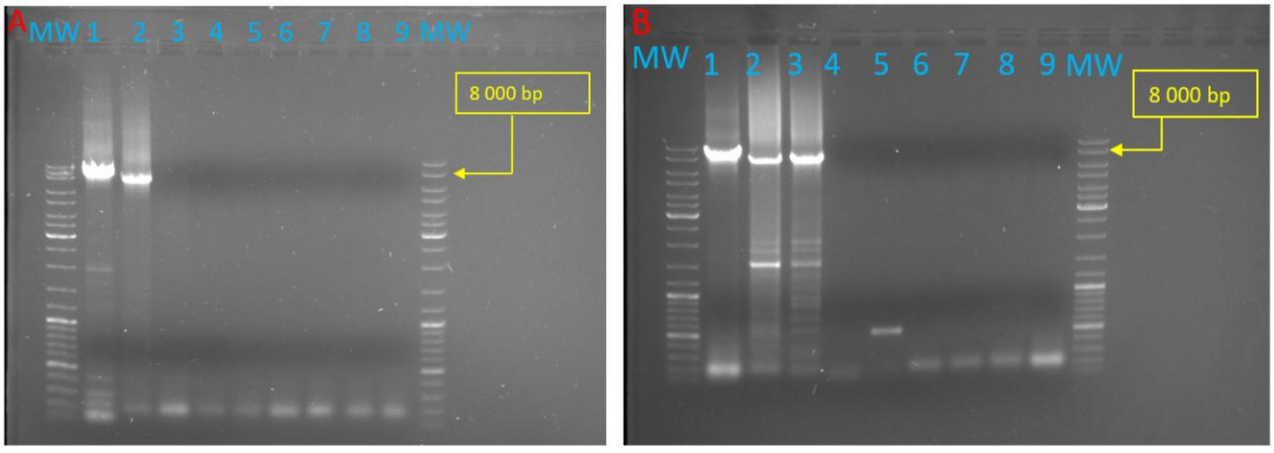

Figure 7A–B. Agarose gel results from qScript and SuperScript IV RT-PCR experiments with CVA9 RNA. 7A, qScript-made cDNAs of CVA9 RNA extracted from purified virus particles were used as templates of Platinum Super Fi II optimal long PCR, RT-primer(s): qScript oligo-dT mix 1X. 7B, same experimental setup as in Figure 5A, but SuperScript IV enzyme used for cDNA generation during RT step, RT-primer(s): Invitrogen oligo-dT_{16}, 50 µM, final concentration 5 µM. Legends: MW, molecular weight marker Gene Ruler Mix 10–10 000 bp, 8 000 bp band highlighted, 1, plasmid control pCVA9-EGFP-6 10^7 copies, 2, $2 \cdot 10^7$ copies, 3, $2 \cdot 10^6$ copies, 4, $2 \cdot 10^5$ copies, 5, $2 \cdot 10^4$ copies, 6, $2 \cdot 10^3$ copies, 7, $2 \cdot 10^2$ copies, 8, no template

control of RT reaction as long PCR template, and 9, long PCR H_2O control. Labels 2–7 on top of the images refer to number of RNA copies added to a single 20 µl RT reaction. 1 µl of the reaction was used as a template in the subsequent 20 µl long PCR reaction by Platinum Super Fi II with x40 PCR cycles. Gel, 0.8 % agarose gel.

In contrast to SuperScript IV RT-PCR products in Figure 7B, the use of Induro Reverse Trancriptase resulted in the cleanest bands on agarose gel when final RT-PCR products were analyzed (Figure 8, A–B).

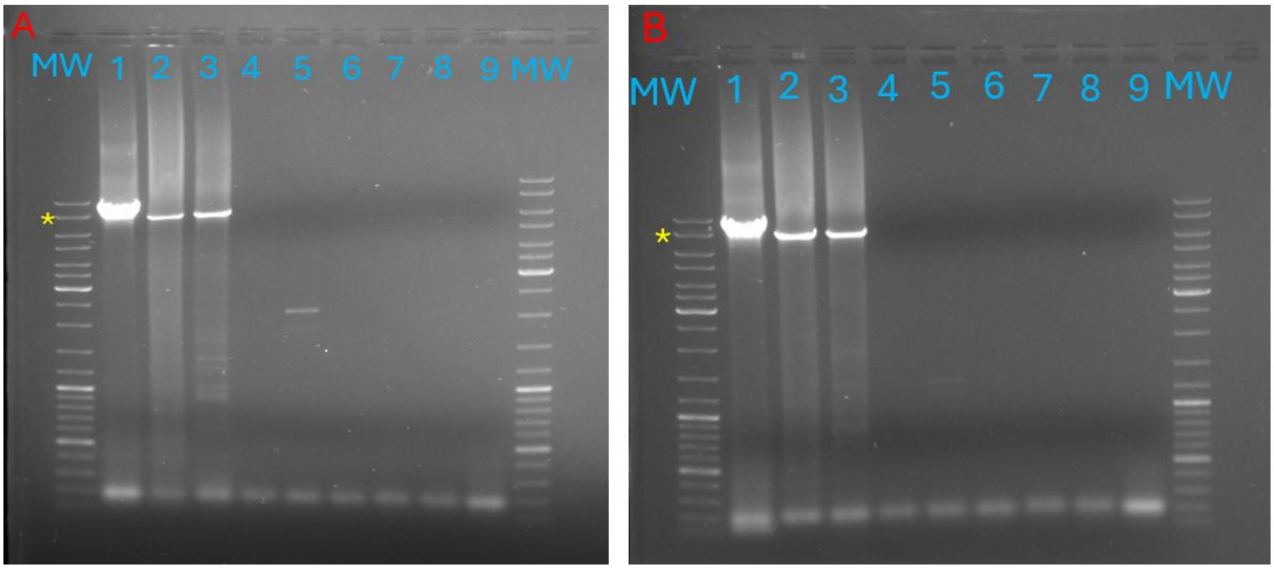

Figure 8A–B. Final products of 2-step Induro RT-PCR on agarose gel. 8A, Induro-RT enzyme used for cDNA generation during RT step of RT-PCR, RT-primer(s): Fermentas oligo-dT_{18}, 100 µM, final concentration 5 µM. Additive: betaine as final concentration of 1 M was added into the RT reaction mix. 8B, same setup but no betaine added. Legends from left to right: MW, molecular weight marker Gene Ruler Mix 100–10 000 bp, 1, PCR positive control, pCVA9-EGFP-6, 10^7 copies, 2, $2 \cdot 10^7$ copies, 3, $2 \cdot 10^6$ copies, 4, $2 \cdot 10^5$ copies, 5, $2 \cdot 10^4$ copies, 6, $2 \cdot 10^3$ copies, 7, $2 \cdot 10^2$ copies, 8, no template control of RT reaction as long PCR template, and 9, long PCR H_2O control. Labels 2–7 in the images refer to RNA copies of extracted CVA9 RNA from purified viruses added to single 20 µl RT reaction. 1 µl of each of the RT reactions was used as a template in the 20 µl long PCR reaction by Platinum Super Fi II (40x PCR cycles). Gel, 0.8 % agarose gel. Legend, *, 8 000 bp band of the molecular weight marker.

In a summary, according to Figures 8A–B, Induro-made cDNAs produced less bands not matching the size of the expected RT-PCR product (CVA9 PCR amplicon, approximate length 7 500 bp) than qScript-made or SuperScript IV-made cDNAs (Figures 7A–B). Especially in Figure 8B, less non-specific bands are seen than in Figure 7B (SuperScript IV RT-PCR products on gel) demonstrating that the RT-PCR products made with SuperScript IV as RT enzyme were probably affected by RNA degradation or non-specific cDNA synthesis during the RT reaction. In the end, by comparing Figures 8A and 8B, no effect of betaine on observed copy number sensitivity ($2 \cdot 10^6$ RNA copies for Induro RT) can be detected.

2.2.2 Applying RT-PCR to full-length amplification of heterogenous samples

Further testing with Induro RT demonstrated excellent performance with RNAs of 7 different CVA9 strains isolated from old cell culture supernatants stored in the virology collection of the University of Turku. Of the 50 µl RNA obtained with E.Z.N.A kit, 1 µl was used for single repetitions of both RT-qPCR and RT-PCR. Before RT-PCR, the quantification by ENRI-RT-qPCR revealed that all the extracted vRNAs were good in integrity and that the copy numbers were sufficient (Table 1) – ranging between 10^4 and 10^6 copies/µl, which matched the desired range.

Table 1. Results of absolute quantification of CVA9 strains by ENRI-RT-qPCR and subsequent full-length 2-step RT-PCR by Induro RT as RT enzyme. The 2 standard samples used in ENRI-RT-qPCR contained 10 000 and 1 000 enteroviral RNA copies/µl against which the experimental samples were compared by qPCR software. RNA sample volume in RT-qPCR, 1.0 µl, RT-qPCR reaction volume, 20.0 µl.

Sample label	Strain / further information	C_q value in RT-qPCR	Calculated concentration (copies/µl) or the standard copy number value of the standard RNAs (copies/µl)	Full-length RT-PCR product visible on agarose gel, +, yes, –, no
1	97-3529	18.28	$4.0 \cdot 10^4$	–
2	61-2740	14.27	$3.3 \cdot 10^5$	–
3	80-11212	13.03	$6.4 \cdot 10^5$	+
4	68-10104	11.98	$1.1 \cdot 10^6$	+
5	59-3192	13.28	$5.6 \cdot 10^5$	+
6	98-2685	12.15	$1.0 \cdot 10^6$	+
7	02-80696	14.56	$2.9 \cdot 10^5$	–
Enterovirus RNA standard 1	Standard containing 10 000 enterovirus RNA copies per 1.0 µl	20.88	10^4	
Enterovirus RNA standard 2	Standard containing 1 000 enterovirus RNA copies per 1.0 µl	25.22	10^3	
RT-qPCR H_2O control sample	Negative result			

Out of the 7 tested isolates in Table 1, 4 produced a positive result on agarose gel when final RT-PCR products were analyzed. These products are visualized in Figure 9. Based on quantification results in Table 1 and final RT-PCR results in Figure 9, it can be estimated that the copy number sensitivity limit is approximately $5 \cdot 10^5$ CVA9 RNA copies/µl for the Induro-based RT-PCR protocol used in this project (see section 4.3.2, RT-PCR schemes).

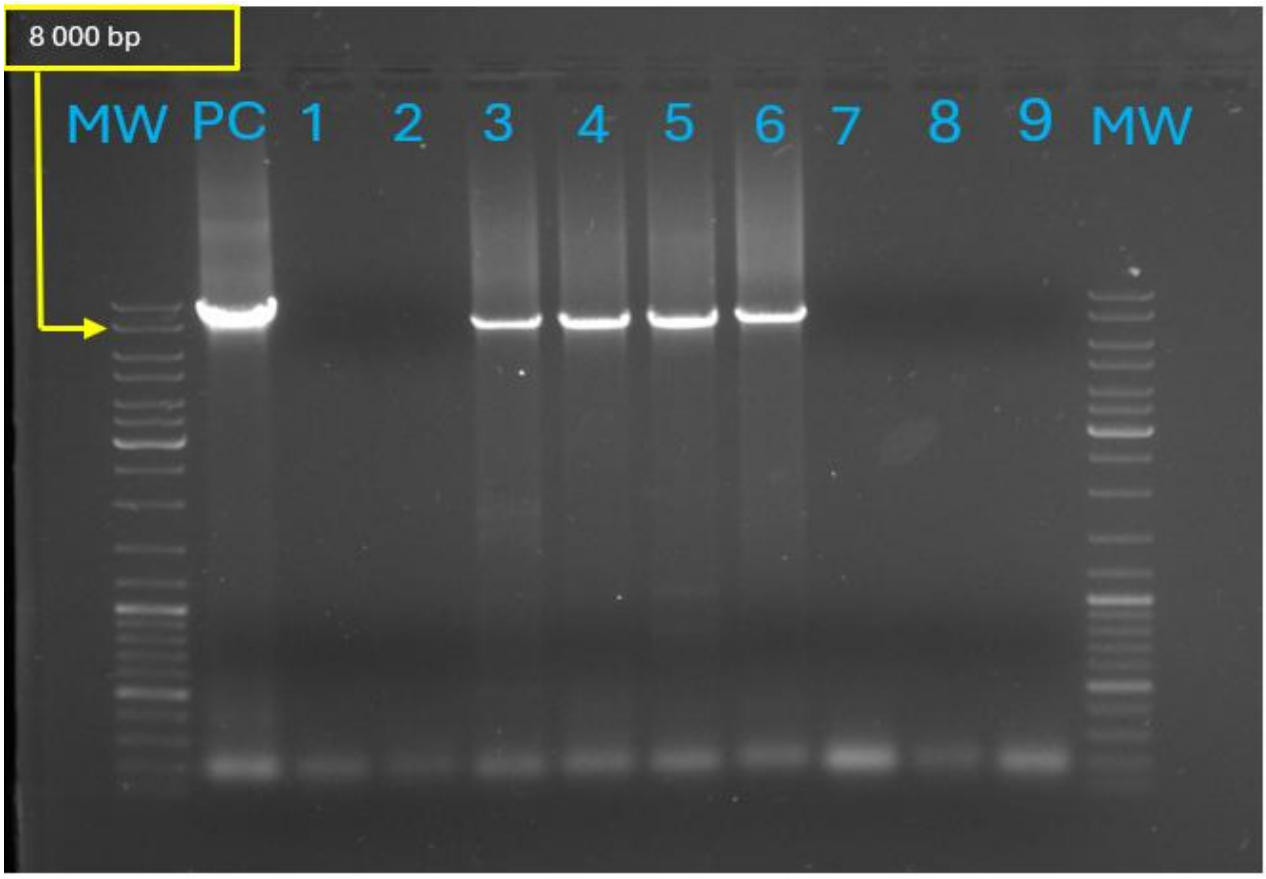

Figure 9. Induro RT-PCR final products made from extracted vRNAs of 7 different CVA9 strains by 2-step RT-PCR protocol. MW, molecular weight marker Gene Ruler Mix 100–10 000 bp, 8 000 bp band highlighted, PC, PCR plasmid control pCVA9-EGFP-6, 10^7 copies. On lanes 1–7 are the RT-PCR products made of the vRNAs of the different CVA9 strains by strain number. 1, 97-3529, 2, 61-2740, 3, 80-11212, 4, 68-10104, 5, 59-3192, 6, 98-2685, 7, 02-80696, 8, RT-H_2O control, 9, PCR-H_2O control. RT-primer(s): Invitrogen oligo-dT_{16} 50 µM, final concentration 5 µM. Gel, 0.8 % agarose. Note, full 20 µl PCR reactions were loaded on the gel. 1.0 µl of each RNA was used per each RT reaction with Induro RT. Subsequently, 1.0 µl of each RT reaction was loaded into 20.0 µl PCR reaction by Platinum Super Fi II (x40 cycles).

According to Figure 9, the bands representing RT-PCR products made of extracted vRNAs of different CVA9 strains were clean, which was expected with fresh sample material. Even though samples of cell culture origin may contain inhibitors of RT reaction or degraded material, Induro RT still managed to generate highly pure cDNA products.

2.2.3 Validation of CVA9-EGFP-6-IVT-RNA as an internal control

In terms of interference with enzymatic reactions, TURBO DNA-*free*™ treatment did not affect RT-PCR or RT-qPCR when DNase-treated IVT-RNA samples were tested several times. The result of the DNase treatment of CVA9-EGFP-6-IVT-RNA sample is in Table 2.

Table 2. The quality control results of a single CVA9-EGFP-6-IVT-RNA (approximate length 8 200 nt) batch treated with 4 U of TURBO DNase™ and 0.2 volume of DNase inactivation reagent. 1.0 volume = volume of DNase digestion reaction (µl). 1.0 µl RNA was used in each 20 µl RT-qPCR reactions. The IVT-RNA was

made from purified PCR products made of pCVA9-EGFP-6 plasmid clone with CVA9gen1 primers and Platinum Super Fi II DNA polymerase (x40 cycles).

Parameter	Result
C_q (RT-positive qPCR replicate)	8.31
C_q (RT-negative qPCR replicate)	29.42
RNA integrity score 0–10 (Qubit™ RNA IQ Assay), 0 = no intact RNA, 10 = 100 % full-length RNA	9.1
RNA concentration measured by Qubit™ RNA HS assay (ng/µl)	25.7
Copy number of RNA (copies/µl)[a]	$5.6 \cdot 10^9$
DNA/RNA ratio[b]	$1 / 2.3 \cdot 10^6$

[a], copy number was calculated by the estimated length of the RNA (8 200 nt), constant factor for molar mass calculations based on RNA length in nucleotides (factor 340 is for RNA), and the measured concentration from Qubit™ experiments in g/µl format (e.g. 1 ng/µl = 10^{-9} g/µl). According to the formula used, molar mass of RNA is 340 · length in nucleotides. [b], DNA/RNA ratio is determined by $2^{-\Delta Cq}$ in which $\Delta C_q = C_{q,\,\text{RT-negative}} - C_{q,\,\text{RT-positive}}$ is based on C_q values from RT-qPCR analysis. It describes to which fraction the amount of the contaminating DNA has decreased in relation to amount of RNA.

In summary, the DNase-treated IVT-RNA was designed to be used as dilutions of 10^7 copies/µl and downwards to 10^0 copies/µl. Accounting for this fact, DNase-treated stock IVT-RNA was to be diluted over 100-fold before using it in sensitive applications, which eliminated the minimal amount of the residual DNA.

2.3 Production of viable viruses in T7-BSR cells

2.3.1 Testing of regulatory primers as quality control step

The regulatory primers (see section 4.4 Regulatory primers and cell-based infection experiments) used in the generation of the PCR products for the transfection experiments were good in integrity according to long PCR results (Figure 10, A–B). In total, 6 different forward and 3 reverse CVA9-specific primers were included in the experimental setup, and 18 different primer pairs formed by combining the 9 said primers were tested with Platinum Super Fi II enzyme before generating PCR products for the transfections (Figure 10, A–B, section 4.4 Regulatory primers and cell-based infection experiments).

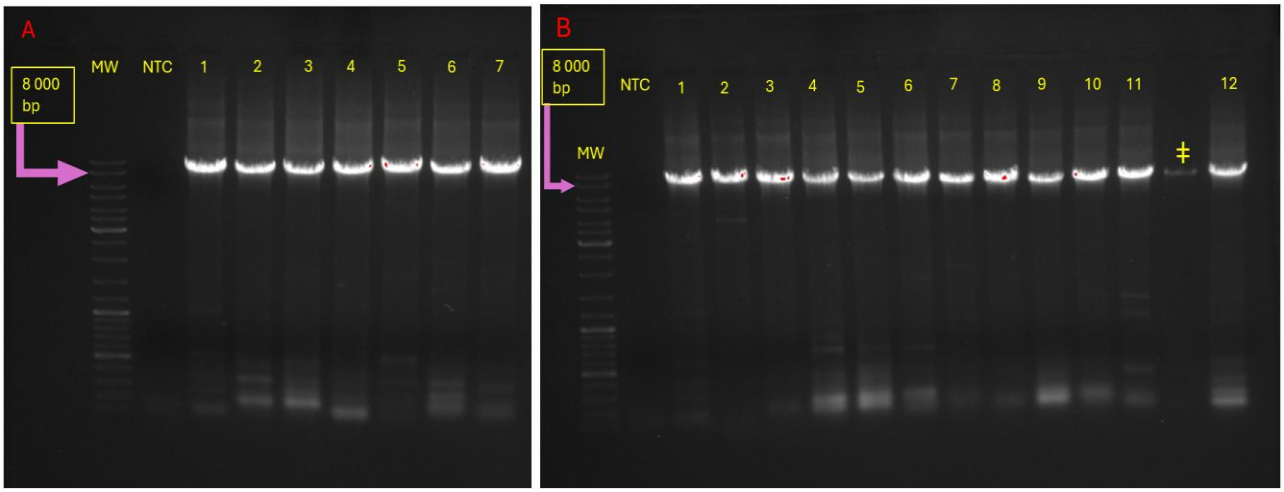

Figure 10. The agarose gel electrophoresis of CVA9-EGFP-6 PCR products made with different regulatory primers and optimized Platinum Super Fi II long PCR protocol (40 cycles) to test primer sets. In both images 10A and 10B, the template used to produce the results was pCVA9-EGFP-6 (10^7 copies per each 20 µl long PCR reaction). The full 20 µl PCR reaction was loaded on the gel. In Figures 10/A–B, NTC, no template control with water instead of DNA template and standard CVA9gen1 (F + R) primers in the reaction mix, and MW, molecular weight marker Gene Ruler Mix 100–10 000 bp, 8 000 bp band highlighted separately. Gel, 0.8 % agarose. Red dots, saturated pixels.

10A. Samples, 1, CVA9gen1 control primers (F + R), 2, T7-CVA9-F-Rz_active + CVA9gen1-R, 3, T7-CVA9-F-Rz_inactive + CVA9gen1-R, 4, TATA-T7-CVA9-F + CVA9gen1-R, 5, TATA-OCTA-T7-CVA9-F + CVA9gen1-R, 6, CVA9gen1-F + CVA9gen1-R-T7_terminator_original, and 7, CVA9gen1-F + CVA9gen1-R-T7_terminator_synthetic.

10B. Samples, 1, CVA9gen1 control primers (F + R), 2, CVA9-Griggs-FL-F + CVA9gen1-R, 3, CVA9-Griggs-FL-F + CVA9gen1-R-T7_terminator_original, 4, T7-CVA9-F-Rz_active + CVA9gen1-R-T7_terminator_original, 5, T7-CVA9-F-Rz_inactive + CVA9gen1-R-T7_terminator_original, 6, TATA-T7-CVA9-F + CVA9gen1-R-T7_terminator_original, 7, TATA-OCTA-T7-CVA9-F + CVA9gen1-R-T7_terminator_original, 8, CVA9-Griggs-FL-F + CVA9gen1-R-T7_terminator_synthetic, 9, T7-CVA9-F-Rz_active + CVA9gen1-R-T7_terminator_synthetic, 10, T7-CVA9-F-Rz_inactive + CVA9gen1-R-T7_terminator_synthetic, 11, TATA-T7-CVA9-F + CVA9gen1-R-T7_terminator_synthetic, and 12, TATA-OCTA-T7-CVA9-F + CVA9gen1-R-T7_terminator_synthetic. Legend, ‡ (in Figure 10B), an artefact caused by minimal amount of liquid spilled over from the well of sample number 11 when the samples were loaded on the gel. All samples are labelled according to the primer pair used in each reaction (forward (F) + reverse (R) CVA9 primers).

In Figure 10, all the PCR products are classified according to the set of primers added to each reaction tube while preparing the long PCR reactions. The main result of the analysis according to Figure 10 (A–B) was that the performance of Platinum Super Fi II remained consistent even though multiple different primer sets were used with the same PCR thermal cycling protocol. This indicates that manufacturer's claim of universal annealing temperature in relation to Platinum Super Fi II is valid. It should be noted that according to Figure 10/A–B, there are no significant differences in product specificity or yield between primer pairs, which demonstrates the high level of the reproducibility required in production of T7 PCR products for transfections.

2.3.2 Viability of T7-BSR cells and transfection efficiency

After transfection, progression of viral infection produced a clearly visible cytopathic effect when the T7-BSR cells were evaluated by light microscopy and fluorescent microscopy at 24 h and 48 h post-transfection. However, the transfection efficiency observed by visual assessment was low throughout the experiments; less than 5 % in most of the repeats, for which not many feasible results were obtained. Regarding T7-PCR amplicons, positive EGFP signal was detected, which was a strong indication of T7RNAP-driven *in vivo* transcription and subsequent translation of viral RNA along with the EGFP insert in the viral clone.

Morphology of T7-BSR cells during the experiments indicated that there was no evidence of instability of the transgene that encodes T7RNAP in T7-BSR cells. When high concentration of geneticin, 500 μg/ml in the medium, was introduced to the cells over several passages, there was still no sign of an increase in the proportion of the dead cells. Based on this fact, it was evaluated that the batch of the T7-BSR cells used in the experiments was stable because cells with unstable transgene would die of geneticin exposure.

When evaluating some of the control plasmids, poor performance was detected. Plasmid pGEM3-GFP with T7 promoter for GFP expression did not produce any fluorescence although purified T7 PCR products did. In addition to this, the plasmid pGFP-7 that was constructed to have a GFP gene under a CMV promoter did not function. Only the performance of pcDNA3-GFP plasmid that had a GFP insert under CMV promoter was feasible according to transfection results. Moreover, CVA9-EGFP-6-IVT-RNA did not produce any fluorescence during the experiments which can probably be explained by RNA degradation.

2.3.3 Detection of GFP signal from the plate

Fluorescence microscopy images (Figure 11, A–F) demonstrate that all the PCR products made for transfections were viable and the CMV promoter-driven plasmid control of transfection, pcDNA3-GFP, was also viable. By comparing Figures 11D and 11E, it is observable that the PCR product made with T7-CVA9-F-Rz_inactive primer as forward primer did not produce any fluorescence, but the product made with T7-CVA9-F-Rz_active as forward primer did. In general, the observations suggest that T7-CVA9-F-Rz_inactive primer is genuinely inactive compared to its active control T7-CVA9-F-Rz_active in context of *in vivo* transcription and virus rescue, but by these images alone this is not determinable.

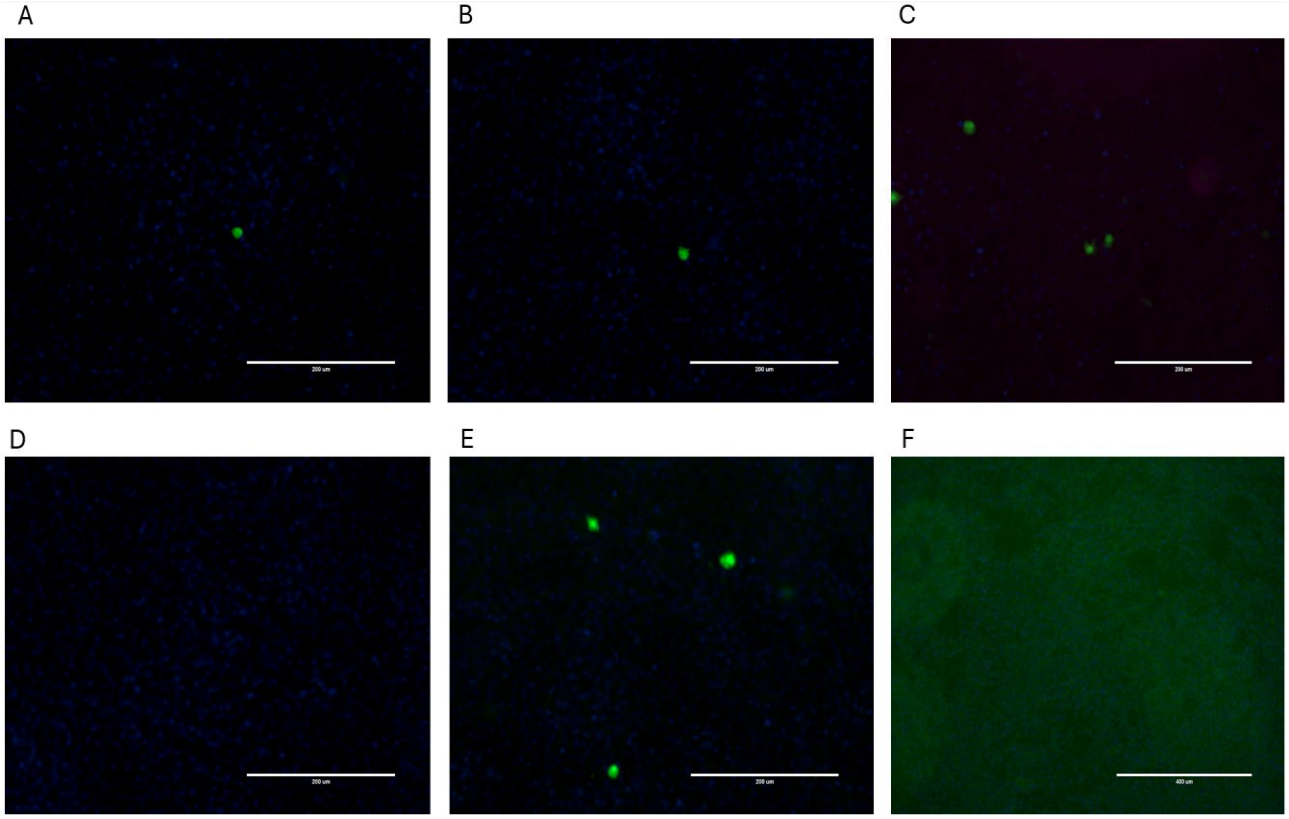

Figure 11, A–F. Merged (DAPI + GFP channels) fluorescence microscopy images of T7-BSR cells fixed 24 h post-transfection on a 96-well black plate at 20 x magnification taken by EVOS FL AUTO system, expect 10F at 10 x resolution. Nuclei were stained with DAPI. The representative images 11A–F were taken of single wells of the plate transfected with different CVA9 clones and PCR products. A, CVA9-EGFP-6-T7-PCR product (made by CVA9gen1 forward and reverse primers), B, pCVA9-EGFP-6 plasmid clone, C, pcDNA3-GFP plasmid control (GFP gene under CMV promoter), D, T7-PCR product CVA9-EGFP-6 (made by T7-CVA9-F-Rz_inactive + CVA9gen1-R primers), E, T7-PCR product CVA9-EGFP-6 (made by T7-CVA9-F-Rz_active + CVA9gen1-R primers), and F, transfection control with water. Scale bars; 11A–11E: 200 µm, 11F, 400 µm. Amount of DNA or PCR product transfected was 100 ng for each well in Figure 11, A–E.

Similar to T7-PCR product-induced fluorescence and viral replication in Figure 11A, PCR products made with either of TATA-T7-CVA9-F or TATA-OCTA-T7-CVA9-F primers as forward primer and CVA9gen1-R as reverse primer in the long PCR reaction produced a single fluorescent focus (Figure 12, A–B) in the transfection experiments. The images in Figure 12 (A–B) were taken of the same plate as in Figure 11, A–F. The transfection control in Figure 11F did not show any fluorescence so the observed fluorescence in other images was estimated to be genuine EGFP fluorescence indicating the occurrence of *in vivo* transcription in the used T7-BSR cells.

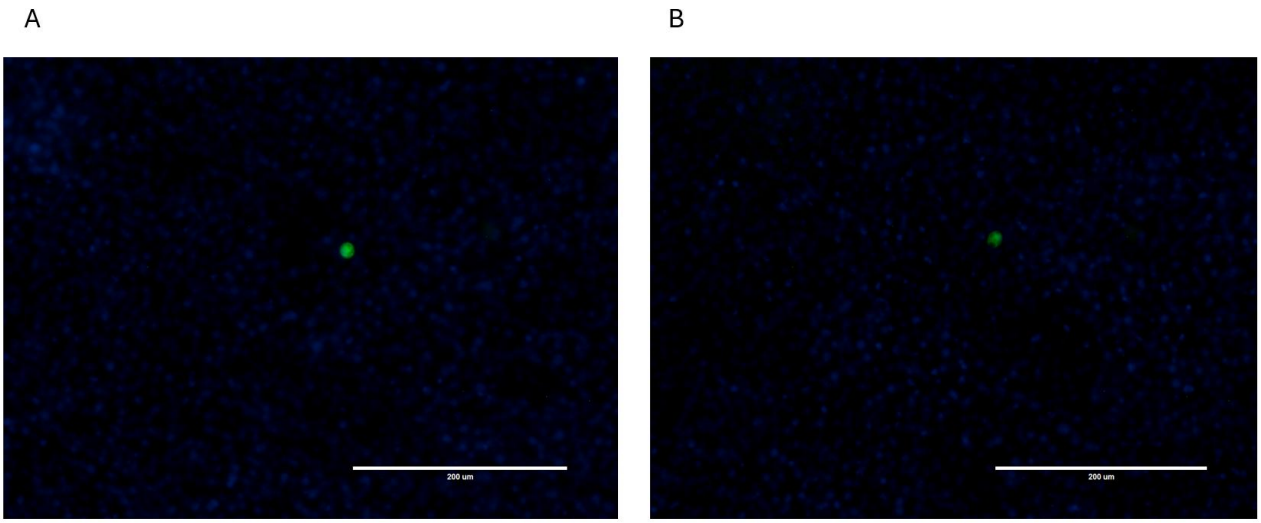

Figure 12, A–B. Merged (DAPI + GFP channels) fluorescence microscopy images of T7-BSR cells fixed 24 h post-transfection on a 96-well black plate at 20 x (A) and 10 x magnification (B) taken by EVOS FL AUTO system. The plate (same as in Figure 11) was fixed 24 h post-transfection and stained with DAPI. (A) T7-BSR cells transfected with CVA9-EGFP-6 PCR product made by TATA-T7-CVA9-F and CVA9gen1-R primers. (B) T7-BSR cells transfected with CVA9-EGFP-6 PCR product made by TATA-OCTA-T7-CVA9-F and CVA9gen1-R primers. Scale bars are 200 µm in Figures 12A and 12B. Amount of PCR product transfected was 100 ng per each well. Both images A and B in Figure 12 represent single wells of a black 96-well plate.

Albeit low transfection efficiency was detected according to Figures 11/A–F and 12/A–B, the observed GFP-positive infection focuses still were a sign of viral infection in T7-BSR cells. By interpreting the images according to information on picornavirus infection cycle, the single infection focuses would contain tens of thousands of mature virus particles. In the context of the viability studies on T7-BSR cells, these results can be considered appropriate and expected.

A549 cells showed no signs of secondary infection when inoculated with a sample from T7-BSR plate (data not shown). This indicated problems in culturing of A549 cells because virus production in T7-BSR cells was successful according to the results and thus no other experiments were performed with the A549 cells.

3 Discussion

3.1 Long PCR and RT-PCR as high-throughput tools in picornavirus research

The ability to produce full-length CVA9 PCR amplicons with a streamlined procedure was a key success factor throughout the project. This enabled the use of only a single plasmid containing the whole CVA9 genome without the need for stepwise cloning. Efficient virus research or vaccine production requires large mass amounts of PCR products, which is a situation difficult to reach by fragment-based approaches. Indeed, the possible instability of the clones created by fragment-based approaches may be a major issue. It has been reported that IVT-RNAs produced from some fragment-based enterovirus clones are not viable in cellular experiments (Yan et al., 2024).

In the context of picornavirus cloning, the compact structure of the genome causes limitations in the insertion of the reporter genes and design of restriction sites. The successful transcription of a linear PCR amplicon into viable vRNA may be dependent on a few nucleotides between the T7 promoter and the viral genome. Therefore, the high fidelity of Platinum Super Fi II enzyme, 300-fold higher compared to traditional derivatives of bacterial *Taq* DNA polymerase according to manufacturer's specifications, can be considered the future of the picornavirus research alongside universal annealing temperature in Platinum Super Fi II protocol. As few genome editing and amplification steps as possible are favored because random mutations may affect the structure of the viral capsid (Yu et al., 2023), which emphasizes that viruses produced from PCR amplicons should be verified via Western blot analysis or electron microscopy as the last resort (Zheng et al., 2009).

According to the PCR results in section 2.1 of this report, the purity of the PCR products was optimal despite the high number, 40, of PCR cycles used. The amount of the product obtained with Platinum Super Fi II was also high compared to repliQa HiFi (Figures 5 and 6). In the context of throughput, it can be estimated that the PCR products were easy to purify via column purification, and thus many well-recognized problems associated with linearized plasmids were avoided. Degraded or unspecific PCR products are known to cause problems in IVT-RNA production, which underlines the potential of the high-fidelity PCR applications tested in this project.

By means of modern PCR, it is possible to introduce precise variable ends with T7 promoter and poly-(A) tail into the PCR product. Therefore, via PCR, different versions of the same plasmid cDNA clone of a picornavirus can be created without having to perform a new cloning step every time. In context of *in vivo* transcription, mutated ends in the PCR products are invaluable tools because they regulate efficiency of T7RNAP-driven transcription. Design of synthetic T7 promoter

sequences which increase the binding affinity of T7RNAP to T7 promoter and stabilize the 3D interactions between T7RNAP and T7 promoter improve efficiency of *in vivo* transcription of PCR products and virus rescue (Bandwar et al., 2002).

In relation to RT-PCR results, according to section 2.2 of this report, the highest observed sensitivity of 2-step RT-PCR was approximately 10^5 CVA9 RNA copies with Induro reverse transcriptase (Figures 8 and 9). This was not concordant with the sensitivity of 10^2 copies of the long PCR phase with Platinum Super Fi II (Figure 5), which can be probably explained by the unique and challenging nature of RT-PCR. Especially the observed stability of produced cDNAs was poor and the RNA was not removed from the cDNAs before PCR phase. The high inhibitor tolerance observed while using Induro RT was considered to indicate that Induro RT would be useful in analysis of clinical enterovirus samples via full-length RT-PCR. In contrast to this, SuperScript IV-made cDNAs produced aberrant bands, and the sensitivity of SuperScript IV was only $2 \cdot 10^6$ RNA copies (Figure 7), which indicated that Induro RT would be the only suitable RT enzyme for future cloning experiments requiring high fidelity. On the other hand, qScript Ultra Flex Kit produced good quality cDNA producing no extra bands on gel in RT-PCR (Figure 7), but the sensitivity was very poor (only $2 \cdot 10^7$ RNA copies). No improvement with betaine additive in Induro RT reaction was obtained for which new additives to improve RT-PCR protocols can serve as potential aims of future research into RT-PCR (Karunanathie et al., 2022). Overall, the Induro-RT protocol was streamlined, and the reaction setup was characterized by hot start formulation of the RT enzyme and fast cDNA synthesis, which significantly simplified the workflow.

3.2 Suitability of long PCR for reverse genetic studies

As a summary, three PCR enzymes – Platinum Super Fi II, repliQa Hifi Tough Mix and Prime Star GXL managed to amplify CAV9 genome with at least satisfactory performance. In comparison to prior evaluations, the sensitivity of 10^2 copies/µl obtained via Platinum Super Fi II was more robust than expected (Figure 5). A significant reduction in time consumption was obtained via Platinum Super Fi II because it did not require adjustments to annealing temperature, which also ensured highly consistent performance throughout all the PCR runs performed.

It was also unexpected that repliQa demonstrated a sensitivity of 10^4 copies/µl when it was accounted for that the repliQa protocol was fast as a long PCR protocol with a thermocycling step lasting less than 1 hour. In the end, Platinum Super Fi II was chosen to be the DNA polymerase included in the 2-step RT-PCR because sensitivity is the most important factor affecting RT-PCR in

which the initial concentration of the sample material may be very low. However, long PCR success factors in reverse genetics experiments are still complicated.

3.3 IVT-RNA production and robust workflow for validation of IVT-RNA controls

Production of feasible CVA9-EGFP-6-IVT-RNA with MEGAscript® kit was challenging. Due to the high amount of pure template PCR product required, extensive long PCR reactions with pCVA9-EGFP-6 template were required. DNA contamination issues and RNA degradation were among the major issues concerning the IVT-RNA production for RT-PCR and RT-qPCR applications. The observed negative results when CVA9-EGFP-6-IVT-RNA was used as a template in RT-PCR were probably related to the contaminating template DNA in the RNA preparation and the annealing of the gene-specific CVA9gen1-R primer to the contaminating template DNA. In downstream applications, appropriate standardization of IVT-RNA preparations is a necessity. Suboptimal IVT-RNA purity, degradation, presence of contaminants or inhibitors of enzymatic reactions and difficulties in storage of IVT-RNA samples are well-recognized issues (Bustin, 2010).

This project aimed at multistep IVT-RNA validation to overcome some of the major issues, which proved to be highly efficient (Table 2). Thus, the successful integration of the different quality control steps into a single validation plan was finally achieved. Firstly, IVT-RNA was produced from purified PCR amplicons that contained no unspecific products or inhibitors of IVT reaction. Secondly, IVT reaction was treated with DNase included in the MEGAscript® kit, and this DNase was removed in column purification. Thirdly, the obtained IVT-RNA was further diluted, rigorously treated with separate TURBO DNA-*free*™ kit and assessed via Qubit™ assays to simultaneously detect quality and concentration. Finally, IVT-RNA was subjected to RT-qPCR to detect presence of contaminating DNA in relation to RNA. All RNA samples were also stored in The RNA Storage Solution, which was considered a success factor throughout the project because modern RNA stabilization agents can even guarantee RNA integrity during several days at +4 °C (McLeish et al., 2012).

3.4 CVA9-EGFP clone and T7 promoter-tagged PCR products in modelling of picornavirus infection

This project achieved some elements of high throughput in modelling picornavirus infection due to advances of EGFP reporter gene insert. In essence, the EGFP insert in the used pCVA9-EGFP clone was integrated into the cleavage site between VP1 and 2A to ensure that translation and expression of the EGFP insert are directly dependent on viral replication which includes cap-independent

translation (Heikkilä et al., 2011). Because of this, the presence of the EGFP fluorescence and the intensity of the fluorescence can act as direct signs of progression of viral infection. This enables real-time and flexible collection of data that is good quality. Real-time monitoring of viral infection can reveal the different mechanisms of the viral lifecycle and spatial information about how the infection spreads in the cell culture. This is an elaborate approach compared to using GFP only as a transfection control or luciferase reporters that have a narrow window of detection (Xu et al., 2015).

During the project, close to all the CVA9-EGFP PCR products were viable in T7-BSR cells, but the transfection efficiency remained low throughout the repeats with the same materials and scheme (Figures 11 and 12). It can be assumed that the chosen method for the transfections might not have been the most optimal considering manufacturer's recommendation that ScreenFect A should be used only in one-step transfections to obtain the best efficiency. In relation to transfected DNAs, PCR products, and RNAs, inaccurate quantification or degradation of RNA templates are potentially significant factors affecting reliability of results. Cell culturing conditions need also to be improved due to unsuccessful A549 culture.

In the context of T7-BSR cells, more validation is required to ensure optimum workflow and to minimize the risk of errors. In future experiments, it would be possible to verify virus production through anti-GFP antibodies, antibodies against viral capsid proteins and sequencing (Li et al., 2020). Production of T7RNAP in T7-BSR cells would also be verifiable through RT-qPCR applications based on those that can detect enterovirus RNA from clinical specimens by designing primers specific to T7RNAP mRNA present in total RNA isolated from T7-BSR cells. Long PCR approach to verify T7RNAP expression via isolated genomic DNA has also been described (Yeong et al., 2021). Cellular morphology during cellular lifecycle and cell culturing conditions may have also affected the results. These factors may affect the viability of cells by modulating cellular protein expression and phenotype. In case of BHK-21 cells from which T7-BSR clone has been derived (Buchholz et al., 1999), there are reports of structure of actin cytoskeleton affecting the replication of enteroviral RNA in the cells (Amadori et al., 1997). Thus, passaging of the cells can affect viral replication, which requires consideration.

Considering the beforementioned success factors of the transfection experiments aimed at virus rescue, the most optimal scheme would include several quality control steps including GFP intensity recordings, anti-GFP antibodies, validated detection of T7RNAP expression, and secondary infections with validated controls (Yeong et al., 2021; Li et al., 2020).

3.5 Future of high-throughput picornavirus research and antiviral drug development

Based on the results of this study, future picornavirus research should be based on high-throughput cloning including long PCR protocols and robust quality control during virus rescue. In context of picornaviruses, robust RT-PCR enables high throughput in sequencing via which the differences between different picornavirus types can be detected. Sequence homologies and point mutations in specific amino acids can serve as direct markers of pathogenicity and viral tropism. However, functional assays with controlled study designs are required to verify the biological significance of the obtained sequence information. In this context, high numbers of different cDNA clones are required.

Induro RT used in this study would be highly beneficial in future cloning experiments due to high fidelity, sensitivity of 10^5 RNA copies and observed high inhibitor tolerance. Oligo-dT primers may offer easy method for cDNA synthesis because poly-(A) tail is a conserved part of picornavirus genome. Direct cloning would be possible by simply extracting gel-purified full-length RT-PCR products and utilizing a suitable plasmid vector for picornavirus studies like previously described (Zheng et al., 2009). Plasmid clones are easily propagated in bacterial cultures, which also increases throughput. Those plasmid vectors are directly amplifiable in PCR which enables streamlined addition of the T7 promoter via PCR primers, which significantly reduces the workload and risk of errors. As a final note, the stability of any plasmid DNA is higher than that of IVT-RNA, which significantly reduces the complexity of the material handling.

Via virus rescue and associated techniques including growth curves and plaque assays, it is possible to determine the functional significance of different picornavirus mutations (Mocé-Llivina et al., 2004). In vaccine and drug development, the identification of the conserved regions or possible target sites for the attenuation of the pathogenic strains are among the most valuable applications.

Transgenic cells with stable T7RNAP expression provide picornavirus research with streamlined opportunities due to simple workflow and high stability of the T7RNAP transgene without toxic effects to cells. In the future, new transgenic cell lines expressing T7RNAP can be constructed via improved precise methods including advanced CRISPR/Cas9 methodologies (Amiri et al., 2023). This would lead to the development of novel cell-based virus rescue models that have good validity in drug development.

3.6 New possibilities of T7RNAP

T7RNAP offers diverse opportunities in virus rescue, which has been the focus of this project. However, on a large scale efficient and versatile T7RNAP constructs are required to improve cost efficiency and quality control of T7RNAP-based experiments. In context of promoters, T7RNAP-driven *in vivo* transcription may be susceptible to incorrect T7 promoter locations in plasmid clones. This emphasizes the need for precise engineering of a plasmid in which T7 promoter, gene of interest, terminator sequence of transcription and the plasmid frame are integrated into a uniform stable construct. This would be beneficial in case of cells expressing T7RNAP because valid transfection controls independent of other promoter regions are required. If a reporter gene construct is bioinformatically and experimentally verified to be only transcribable by T7RNAP, the reporter gene in question under T7 promoter can serve both as a transfection control and a validator of the cell line used as described previously (Fu et al., 2021).

Synthetic promoter regions are helpful in virus rescue because virus rescue is an expensive procedure and high mass amounts of viruses are hard to produce in cells for downstream purposes. It has been described earlier that T7RNAP expression in cells secures high virus titer in enterovirus rescue (Fu et al., 2021).

In relation to T7RNAP, the enzyme is prone to read-through transcription unless exact terminator sequences are inserted into the constructs to be used with T7RNAP expression systems. Bioinformatically designed new terminator sequences offer novel benefits since the possibility of the read-through transcription drops to under 1 %, which is especially important with plasmid constructs (Mairhofer et al., 2015).

3.7 Final conclusions

The purpose of this research project was to rescue CVA9 from EGFP-bearing clone by T7-BSR cells, which was achieved. The results demonstrate that significant simplification of picornavirus research is possible via long PCR and T7 promoter system. *In vivo* transcription is also a cost-efficient option compared to IVT-RNA production. Real-time EGFP signal detection has several advantages over traditional methods: Only fluorescent microscopy is required and there is no need for complex staining steps, washing or antibody incubations. In addition, real-time imaging enables continuous detection of virus infection in living cells whereas antibody-based methods are dependent on only single measurements with fixed cells and provide no coverage of full viral

infection cycle. Thus, functional assays including the detection of the virus internalization benefit from the EGFP construct used in this project.

Quality control in virus research is also a major issue pertaining to long PCR, RNA work and cell-based experiments. Fluorometry-based detection assays are especially valuable while working with sensitive RNA samples, and traditionally the information about RNA integrity has been obtained via agarose gel electrophoresis which is time-consuming and may involve dangerous chemicals.

RT-PCR needs validation in the future because more information about the success factors is required for development of universal RT-PCR protocols for picornaviruses. According to some of the results, prepared cDNAs were sensitive to effects of storage so fast workflow in RT-PCR is recommended.

Overall, full-length RT-PCR of picornaviruses is still an evolving concept even though the first reports appeared almost 30 years ago (Lindberg et al., 1997). Not only the effective RT-PCR enables streamlined sequencing, but also the opportunities created by genetic information. Exact information is required when PCR primers and suitable mutagenesis sites are engineered. Improvement of sensitivity of full-length RT-PCR is important in the future, because diagnostic ENRI-RT-qPCR has a detection limit of approximately 10^2 RNA copies, and clinical specimens are known to contain low amounts of vRNA (McLeish et al., 2012).

In the drug development sector, effective virus rescue techniques would enable characterization of virus clones with different functions via EGFP, and accurate 3D drug design based on sequence and crystallography information on protein structure (Lyu et al., 2015; Heikkilä et al., 2011). The main idea of the combination of long PCR, EGFP reporter gene, and *in vivo* transcription is to reduce the workload because with only a few steps the risk of any errors is drastically reduced. Statistically significant results are also easy to obtain with high-throughput methods. Continuous combination of improved materials and methods is the key to success because no single technique itself is enough.

4 Materials and methods

4.1 Plasmids and RNAs used

4.1.1 Plasmid specifications

Plasmids containing either CVA9 genome with and without the EGFP reporter gene insert or the gene coding for T7RNAP with either CMV promoter composition or dual CMV-T7 promoter composition were used. They were obtained from the laboratory storage and were previously prepared but not sequenced.

Table 3. An overview of the plasmids containing viral cDNAs or T7RNAP gene as an insert.

Plasmid name	Inserted cDNA or genomic constructs – length of insert is given in bp without plasmid frame (if known)	GeneBank code (if available)	Reference
pCVA9	Full coxsackievirus A9 genome, 7 452 bp	D00627	(Chang et al., 1989)
pCVA9-EGFP	Full coxsackievirus A9 genome with EGFP reporter gene insert between VP1 and 2A sites, approximately 8 200 bp in length		(Heikkilä et al., 2011)
T7RNAP-CMV	T7RNAP gene, only CMV promoter		(Brisson et al., 1999)
T7RNAP-CMV-T7	T7RNAP gene, dual promoter T7-CMV in the same plasmid		(Brisson et al., 1999)

The concentrations [ng/µl] of the stock plasmids from the virology collection were verified by virtue of spectrophotometry with DeNovix DS-11 Spectrophotometer instrument (DeNovix Inc.). Copy number calculations with the CVA9 plasmids assumed that the molecular weight (*MW*) of the full plasmid including the CVA9-cDNA insert was 10 000 bp. The following formula was used to

calculate copy number Q per 1 µl (PCR sample volume) for double-stranded DNA: $Q = \frac{c[\frac{g}{\mu l}]}{MW\ [\text{length of plasmid in bp}] \cdot 660} \cdot 6.022 \cdot 10^{23}\ \frac{1}{\text{mol}}$ in which the factor $6.022 \cdot 10^{23}$ [(number of particles/molecules) / mol] is the Avogadro constant and Q is the copy number per 1 µl in this equation. A RT-qPCR protocol involving previously prepared commercial enterovirus vRNA standard samples (VirCell, Spain) as controls with adjusted copy numbers was used to verify that dilution factors were correct. The pCVA9 and pCVA9-EGFP plasmids were used as 10-fold dilutions from 10^7 copies/µl to 10^0 copies/µl prepared in Tris/HCl buffer solution (pH = 8.5).

4.1.2 Sequencing of plasmids and verification of integrity

A commercial service provider (Eurofins Ltd., Cologne, Germany) was used to obtain sequencing information on the plasmids described in Table 3. Based on obtained sequencing reports, the quality of the plasmids was evaluated. The presence of correct T7 promoter regions, initiators of translation, genomic insertions, terminator sequences, and the reading frame were verified.

4.1.3 RNA samples, production and extraction

CVA9-EGFP-RNA was used as a reporter gene construct for cell-based infection experiments so that EGFP as a permanent insert of the viral genome would produce fluorescence during infection. The tested CVA9-EGFP-RNA samples were either old *in vitro* transcribed RNAs (IVT-RNAs) from the virology collection of the laboratory or newly prepared IVT-RNAs synthetized directly from linear PCR products by virtue of high-quality MEGAscript® T7 *in vitro* transcription (IVT) kit (catalogue code AM1333, Thermo Fisher Scientific). The synthesized IVT-RNAs were treated with TURBO DNase™ included in the MEGAscript® kit for 1 h immediately after the IVT reaction to remove the most significant traces of the residual template DNA present in the IVT reaction mix. In addition, the degradation of the contaminating template DNA was later verified by template-specific RT-qPCR. The amplification curves produced by the replicated RT-qPCR reactions of the purified IVT-RNAs containing either added RT enzyme mix or not were compared to each other to assess removal of contaminating DNA.

The TURBO DNase™ was removed from the initial IVT reaction by purifying the produced IVT-RNA with MEGAclear™ filter cartridge kit for high-yield RNA specimens (catalogue code AM1908, Thermo Fisher Scientific). Linear PCR product that was used as a template for the IVT reaction was generated by using the prior-made, purified CVA9-EGFP-6 plasmid from the virological specimen collection as a template while Platinum Super Fi II long PCR enzyme was

used in the PCR reaction (see section 4.2.2). Linear PCR amplicons were purified by silica membrane filter cartridges included in NucleoSpin® Gel and PCR Clean-up kit (catalogue code 740609.50, MACHEREY-NAGEL, Düren, Germany). Purified and non-purified controls of linear PCR products were also subjected to agarose gel electrophoresis before IVT reactions were performed. Further DNA removal of diluted and purified IVT-RNA products was performed by using specialized TURBO DNA-*free*™ kit (Thermo Fisher, catalogue AM1907) to obtain the highest quality IVT-RNA for downstream applications in which a few copies of contaminating DNA would be detrimental. The DNA-*free*™ kit included a chemical inactivator enabling the inactivation of the DNase in the sample without column purification or other special purification protocol. All samples were initially analyzed by the spectrophotometer DeNovix DS-11 to determine concentration for downstream analysis.

In addition, IVT-RNA samples were analysed by Qubit™ assays to confirm integrity (Qubit™ RNA IQ Assay, catalogue Q33221, Thermo Fisher) and to measure concentration (Qubit™ RNA HS Assay, input range 5–100 ng, catalogue Q32852, Thermo Fisher) fluorometrically to further optimize the experiments in selected cases. The specified Qubit™ assays removed the need for the extended RT-qPCR or similar complex procedures while assessing the RNA samples. Precise quantification was applied so that DNase-treated IVT-RNA was used to construct an internal standard series of robust quality.

An aliquot of CVA9 RNA for the long RT-PCR experiments was obtained by extracting it from old infectious virological specimens or purified virus particles. These sources were guaranteed not to contain any viral cDNA or transfection-specific material. The extraction was performed by E.Z.N.A.® Viral RNA Kit (catalogue R6874, OMEGA Bio-Tek). In the scope of the experiments performed, the extracted CVA9 RNA was used to ensure high throughput due to time-consuming DNA removal processes in case of IVT-RNA. E.Z.N.A kit was also used to isolate different CVA9 strains from cell culture samples. All RNA samples were stored in nuclease-free water or specific sodium citrate buffer for RNA named The RNA Storage Solution (catalogue AM7000, Thermo Fisher). All the samples were obtained from the virology collection of the University of Turku.

4.1.4 Agarose gel electrophoresis and quality control of PCR products

All PCR products and associated no template control samples (NTCs) were run on a non-denaturing 0.8 % agarose gel (w/V) prepared in the 1 x tris-acetate buffer. In all cases, the full 20 µl PCR or RT-PCR reaction was used in agarose gel experiments after thermocycling. Samples were loaded on the gel by either 6 x DNA Gel Loading Dye (catalogue R0611, Thermo Fisher) or 6 x Tri Track

DNA Loading Dye (catalogue R1161, Thermo Fisher). Fluorescent dye for visualization of DNA bands was included in the gel solution in concentration of 5 µl stain per 100 ml gel solution (Midori Green Advance DNA stain, Nippon Genetics). GeneRuler DNA Ladder Mix, ready-to-use (catalogue SM0333, Thermo Fisher Scientific) suitable for sizing of 100–10 000 bp bands was utilized as a molecular weight marker in the agarose gel experiments. To obtain accurate separation of bands, all gels were run at 100 V until the loading dye front had reached the end of the gel. All agarose gels were imagined by BioRad Gel Doc XR+ system (BioRad Laboratories Inc.) attached to a computer with Image Lab software (BioRad Laboratories Inc.). The obtained gel images were then processed with PowerPoint (Microsoft).

4.2 Standard long PCR enzymes and PCR parameters

4.2.1 Primers

CVA9-specific standard CVA9-gen1 forward primer with a T7 promoter and reverse CVA9gen1-R primer with a poly-(A) tail from the laboratory collection were used in the long PCR and copy number sensitivity testing (Table 4). The melting temperature of the annealing part of the primer was calculated by using Thermo Fisher T_m calculator. These primers are referred to as standard or control CVA9 primers because they contain only a T7 promoter and a poly-(A) tail but not any regulatory elements.

Table 4. The standard primers for amplification of CVA9 cDNA in long PCR. Melting temperature T_m of part complementary to CVA9 cDNA is also presented. Legends, F, forward, R, reverse for primers.

Primer label	Sequence (annealing part complementary to CVA9 genome is enclosed with parenthesis)	T_m (°C)	GC content of part complementary to CVA9 sequence (%)
CVA9-gen1-F – contains also T7 promoter flanking the 5'-end before CVA9-annealing part	5'-TAATACGACTCACTATAGGG(TTTAAAACAGCCTGTGGGTTGTTCCC)-3'	68.8	46.2
CVA9-gen1-R with	5'-TTTTTTTTTTTTTTTTTTTT(CCTCCGCACCGAATGCGG)-3'	68.7	72.2

poly-A tail			

This primer set with the T7 promoter in the forward primer was also used in producing PCR amplicons for IVT-RNA production and transfections because T7 promoter can be directly read by T7RNAP in transgenic cells.

4.2.2 High-fidelity long PCR enzymes

In total, 6 different DNA polymerases designed for long PCR were tested with CVA9 cDNA plasmid clones so that the sample copy numbers were varied. The basis for the long PCR protocols and their adjustments have been previously described in Koskinen (2023).

Table 5. Description of enzymes used in long PCR of CVA9-templates. Hot start refers to possibility of reaction setup at room temperature – i.e. the DNA polymerase is only activated during PCR thermocycling.

Name of the DNA polymerase / long PCR kit	Special notes according to manufacturers' manuals	Manufacturer	Manufacturer's catalogue number
Platinum SuperFi™ II	Hot start, up to 20 kb targets, recommended universal annealing at 60 °C due to stabilizers in reaction buffer Suitable for targets with up to 75 % GC content	Thermo Fisher Scientific	12361010
repliQa HiFi ToughMix 2X	Amplification of maximum 24 kb genomic targets, robust and inhibitor resistant	Quantabio	95200
KAPA HiFi HotStart DNA Polymerase	Maximum 20 kb targets of non-genomic DNA accepted, and hot-start formulation	KAPA Biosystems	07958889001
Q5 Hot Start High-Fidelity DNA polymerase	Hot start technology, very high fidelity	New England Biolabs	M4093
Phusion HotStart II High-Fidelity DNA Polymerase	Improved fidelity, special formulation	Thermo Fisher Scientific	F549S
PrimeStar GXL	High fidelity, suitable for at least 30 kb targets	TAKARA BIO	#R050A

All the enzymes listed in Table 5 were used according to the best practices described in the respective manuals. The prepared pipetting chart is given as Table 6. However, some modifications were implemented to ensure high enough yields with long PCR products in relation to the fact that CVA9 cDNA is approximately 7 500 bp long and CVA9-EGFP cDNA approximately 8 200 bp. A standard 20 µl reaction volume was applied in each case in which copy number sensitivity analyses, production of PCR amplicons, primer testing or other forms of cDNA analyses were conducted. Only CVA9 cDNA clone pCVA9-1 without EGFP insert was used as the template in copy number sensitivity analyses.

Table 6. Standard pipetting chart describing the full protocol applied to the long PCR and copy number sensitivity analyses.

Component/reagent label (stock concentration)	Volumes (µl) for each enzyme/kit (final concentration in parenthesis if known)					
	Platinum Super Fi II	KAPA HiFi	Phusion HotStart II	repliQa HiFi Tough Mix	PrimeStar GXL	Q5
Nuclease-free water	12.2	12.8	12.4	7.8	11.4	12.4
5X reaction buffer (all but repliQa) or 2X ready master mix (MM), only repliQa	4	4	4	10	4	4
CVA9-gen1-F primer (10 µM)	1 (0.5 µM)	0.6 (0.3 µM)	1 (0.5 µM)	0.6 (0.3 µM)	0.6 (0.3 µM)	1 (0.5 µM)
CVA9-gen1-R primer (10 µM)	1 (0.5 µM)	0.6 (0.3 µM)	1 (0.5 µM)	0.6 (0.3 µM)	0.6 (0.3 µM)	1 (0.5 µM)
Premixed 10 mM each or 2.5 mM each dNTPs	10 mM, 0.4 (0.2 µM)	10 mM, 0.6 (0.3 µM)	10 mM, 0.4 (0.2 µM)	N/A, 2X MM includes these	2.5 mM, 1.6 (0.2 µM)	10 mM, 0.4 (0.2 µM)
Kit-specific DNA polymerase	0.4	0.4 (0.02 U/µl)	0.2 (0.02 U/µl)	N/A, 2X MM includes these	0.8 (0.05 U/µl)	0.2 (0.02 U/µl)
Template DNA	1					
Total volume	20					

The PCR cycling was designed so that the maximum amount of the product should be obtained so that the signal representing the specific DNA band obtained via the UV imaging of the agarose gel demonstrated the highest intensity possible. The PCR cycling was also modified to the extent recommended in manufacturers' product manuals to optimize the yield of the long targets because, for example, CVA9 PCR products have a length of over 7.4 kbp. The optimized PCR cycling programs are described in Table 7.

Table 7. Optimized PCR cycling for different enzymes when pCVA9-1 was the template used (target size approximately 8 kbp). Enzyme name abbreviations in this table: KAPA HiFi (KH), Q5, Prime Star GXL

(PSGXL), Platinum Super Fi II (PSFII), repliQa (RQ), and Phusion HotStart II (PHII). Optimization of parameters was partly based on work by Koskinen (2023).

PCR cycling protocol master sheet			
Step[e]	Temperature	Time	Number of cycles[a]
Initial denaturation (applied only to KH, PSFII, Q5, and PHII protocols)	98 °C, expect KH at 95 °C	60 s (PSFII), 30 s (Q5 and PHII), 3 min (KH)	1
Denaturation	98 °C	15 s for PSFII, 10 s for RQ, PHII, Q5 and PSGXL, 20 s for KH	35 (RQ, Q5, KH and PHII), 40 (PSGXL, PSFII)
Annealing[b]	60 °C (PSGXL)	20 s, expect 15 s for KH and PSGXL	
	67 °C (KH, PSFII, and PHII)		
	70 °C (Q5)		
Extension[c]	72 °C for all expect with RQ at 68 °C	40 s (for RQ, combined annealing and extension only)	
		4 min (PSFII, PHII)	
		5 min 30 s (Q5)	
		6 min (KH)	
		7 min 30 s (PSGXL)	
Final extension[d] (only applied to PSFII, KH, PHII, and Q5)	72 °C	2 min (Q5)	1
		7 min 30 s (PSFII)	
		8 min (PHII, KH)	
Hold	4–10 °C	∞	

[a], an upper limit of cycles, 35 or 40, was set to prevent non-specific products from being amplified. [b], annealing temperature was based on the characteristics of the primers, but repliQa, PrimeStar GXL, Q5, and Platinum Super Fi II do not follow standard annealing rules due to their unique product formulations. RepliQa was used with 2-step cycling with no annealing phase. [c], the duration of the extension depends on the length of the target in relation to the enzyme-specific speed of the synthesis to ensure the optimum amplification of the long ≥5 kb targets so that the 30–60 s/kbp of the product is the basic formula. [d], in some cases, final extension was included to ensure the highest PCR performance and product yield. [e], unless otherwise specified, all the parameters were constant among all kits tested. Variations are indicated by enzyme names when relevant.

In Table 7, Q5 protocol had an annealing temperature 3 °C higher than the standard 67 °C due to high salt buffer of Q5 – this was set according to manufacturer's instructions.

4.3 RT-PCR and RT-qPCR

4.3.1 Overview of qPCR practices

To ensure efficient and constant quality control during this project, RT-qPCR and qPCR with no RT enzyme were used to validate RNA samples by detecting DNA contamination and to verify copy

number series. Prepared samples were tested against enterovirus RNA copy number standards. The qPCR primer system was based on reverse (4–) and forward (3+) entero-rhino (ENRI) primers that bind to a specific conserved subregion located in the UTR of the 5' end of the genomes of both the human enteroviruses and rhinoviruses. These ENRI primers (Table 8) were also used to quantify the plasmid cDNA clones used in long PCR and to analyze cDNAs produced in RT-PCR experiments.

Table 8. The characteristics of the ENRI primers utilized in the RT-qPCR and qPCR experiments.

Label	Nucleotide sequence of the primer	T_m (°C)	References
ENRI, reverse, 4–	5´-GAAACACGGACACCCAAAGTA-3'	57.9	(Österback et al., 2013) (Lönnrot et al., 1999)
ENRI, forward, 3+	5´-CGGCCCCTGAATGCGGCTAA-3'	63.5	

The primers described in Table 8 were used in conjunction with the following two RT-qPCR kits based on SYBR Green dye chemistry. QuantiNova SYBR Green RT-PCR Kit (catalogue 208152, Qiagen) and KAPA SYBR Fast One-Step RT-PCR Kit (KAPA Biosystems) were kits designed for one-step RT-qPCR in which RT reaction and subsequent cDNA amplification during PCR are combined in a single reaction tube. Adjusted reaction protocols are given in Tables 9 and 10.

Table 9. The tested no-probe RT-qPCR reaction scheme. The 20 µl reaction volume was chosen as the standard volume into which various samples adjusted to contain desired copies in 1.0 µl volume were added.

Reaction volumes (µl)	
Component label	Volumes (µl) and final concentration in parenthesis
RNase-free water	6.8^{Q} or 7.0^{K} for RT-positive reactions and 7.0^{Q} or 7.4^{K} for RT-negative reactions
ENRI3+ 10 µM stock	1.0^{Q} (0.5 µM) or 0.8^{K} (0.4 µM)
ENRI4– 10 µM stock	1.0^{Q} (0.5 µM) or 0.8^{K} (0.4 µM)
2x QuantiNova SYBR Green or 2x KAPA SYBR Fast master mix	10.0 (1x)
Separate 40 x KAPA or 50 x QuantiNova RT mix added to RT-positive reactions	0.2^{Q} or 0.4^{K} (final concentration 1x)
vRNA template, produced cDNA or plasmid clone	1.0
Total volume	20.0

^{Q}, QuantiNova SYBR Green, and ^{K}, KAPA SYBR Fast.

The RT-qPCR program used with a qPCR machine is given in Table 10.

Table 10. Thermal cycling used in RT-qPCR experiments.

Thermal cycling of RT-qPCR			
Phase		Temperature (°C)	Time
RT step	RT reaction[a]	50[Q] or 45[K]	10 min
	Inactivation of RT enzyme and activation of DNA polymerase	95	2 min[Q], 3 min[K]
3-step PCR cycling x40	Denaturation	95	15 s
	Annealing	Touchdown from 65 °C to 56 °C by 1 °C increments 9 times or constant temperature equaling T_m of ENRI4– ≈ 58 °C	10–20 s
	Extension and signal acquisition (FAM or SYBR Green setting, green channel)	72	5–10 s

[Q], QuantiNova SYBR Green, and [K], KAPA SYBR Fast. [a], when assessing only cDNAs via qPCR, the RT step and/or RT enzyme was omitted.

Copy number calculations were based on log2 scale by virtue of which the relationship between sample copy numbers c_1 and c_2 and corresponding cycle of quantification values (C_q) can be described by an equation $\frac{c_2}{c_1} = 2^{-\Delta c_q}$. In this equation, ΔC_q is the difference in measured C_q values between sample copy numbers c_1 and c_2. Of note, $\log_2 10 \approx 3.32$ is a mathematical condition which demonstrates that approximately |3.3| C_q units describe a 10-fold difference in sample copy number if amplification efficiency is assumed to be 100 %. Melt curve analysis in the qPCR software was also performed to assess possible formation of non-specific products to detect contamination. Amplification efficiency between experiments was compared by using qPCR device software to detect possible template degradation. The experiments were performed with Rotor Gene Q (Qiagen) or Mic Real Time PCR Cycler (Bio Molecular Systems) real-time PCR instruments. Amplification efficiency of PCR can be described by an equation $N_x = N_y \cdot E^k$ in which N_x is the number of PCR product molecules after $k = x - y$ cycles of amplification, the starting point of which is N_y (number of molecules at the starting point when y cycles has passed). If the factor E is exactly 2, then the amount of PCR product is doubled during each cycle, and the amplification follows perfectly log2 mathematics. In addition, if E is exactly 2, the amplification efficiency is 100 %, and if E is 1, the efficiency is 0 % (E in the equation can be any value between 1 and 2 (no unit)). When this is scaled, 100 % efficiency corresponds to value 1, and thus a value of 0.90, for example, corresponds to E of 1.80 (90 % PCR efficiency) according to the equation. In this project, the latter scale was used, and range [0.90; 1.10] of values was used as an indication of good PCR efficiency and

template quality – in actual analyses, up to 110 % efficiency values are accepted to account for presence of small real-world uncertainty always present during signal acquisition (Ruijter et al., 2009).

4.3.2 RT-PCR schemes

RT-PCR was based on using RT enzymes specifically designed for long and difficult targets. Total first strand cDNA synthesis was chosen as a rational basis for the technical specifications of the reactions performed. Synthesized cDNAs were immediately used as templates in long PCR (see section 4.2) by including 1 µl of cDNA reaction mix from 20 µl RT reaction into the 20 µl PCR reaction (ratio 1/20). The PCR amplicons were then analyzed on agarose gel to demonstrate the capability of the RT enzyme to produce viable and full-length cDNA that was amplifiable via long PCR. The number of RNA copies added to the RT reaction was the parameter chosen for representing the sensitivity of the final version of the 2-phase RT-PCR protocol. The overview of the RT enzymes tested is disclosed in Table 11.

Table 11. The overview of the RT enzymes tested in terms of their performance in long-range RT-PCR.

Manufacturer	Product label	Catalogue code	Short description of performance according to manufacturers' data sheets
Thermo Fisher Scientific	SuperScript IV	18090010	Up to 12 kb targets in 10 minutes
New England Biolabs	LunaScript RT master mix, primer-free	E3025	Up to 9 kb in 10 minutes, reaction setup at room temperature possible
New England Biolabs	Induro Reverse Transcriptase	M0681	Up to 20 kb in 10 minutes, reaction setup at room temperature possible
Quantabio	qScript Ultra Flex kit	95215	Up to 20 kb targets in 10 minutes

All enzymes in Table 11 were subjected to variable primer sets. First-strand cDNA synthesis was performed either with gene-specific reverse CVA9gen1-R primer or oligo-dT primer specific to the poly-(A) tail 3' end of picornavirus genome according to the kit instructions. The rationale behind this was to control the quality of the different cDNAs by ENRI-RT-qPCR (see section 4.3.1) or by detecting non-specific products or smearing on agarose gel while using prepared cDNAs as templates of long PCR reaction according to section 4.2. Detailed testing was performed to detect the products of suboptimal quality. Amplification efficiency values between 0.90 and 1.10 were used as an indicator of good product quality when ENRI-RT-qPCR results were analyzed.

After initial testing with limited copy number series, the most feasible RT enzymes and primer sets were subjected to 20 µl reverse transcription reactions in high-throughput assays. In the first instance, these assays involved a 10-fold dilution series of extracted CVA9 vRNA from copy number of $2 \cdot 10^7$ copies/µl down to $2 \cdot 10^2$ copies/µl. The dilution series was prepared to guarantee standardized cDNA copy number in the reaction mix for the subsequent PCR amplification assuming 100 % RT step efficiency. In the end, both *in vitro* transcribed CVA9-EGFP-6-RNA and RNAs purified from cell lysates or samples containing purified virus particles were utilized in the RT-PCR experiments. The detailed protocols for each RT enzyme are disclosed in Tables 12–15. Note that in oligo-dT_x primer label the number x signifies the length of the oligo-dT primer used.

Table 12. Protocol for Induro reverse transcriptase. Note that separate and combined annealing-denaturation step was performed with RNA-primer mix before adding enzyme mix.

Pipetting chart			Thermal cycling for RT		
Component	Notes	Volume, µl (final concentration in the reaction)	Step	Time	Temperature (°C)
5x RT buffer	Enzyme mixture	4.0 (1x)	Primer annealing	5 min	65
RT enzyme (200,000 U/ml)		1.0 (10 U/µl)	Cooling on ice	≥1 min	
RNasin Plus Ribonuclease Inhibitor (40 U/µl), catalogue N261A (Promega)		0.2 (0.4 U/µl)	Reverse transcription[a]	30 min	57
Betaine[b] 5 M		4.0 (1 M)			
Water		to 10.0			
dNTPs, 10 mM each, catalogue #N0447 (New England Biolabs)	Primer annealing mixture	1.0 (0.5 mM each)			
Gene-specific CVA9-gen1-R primer 10 µM, Invitrogen oligo-dT_{16} 50 µM or Fermentas oligo-dT_{18} 100 µM		1.0 (0.5 µM, gene-specific), 2.0 or 1.0 (oligo-dT, final concentration 5 µM)	Inactivation of RT enzyme	1 min	95
Water		to 9.0			
Template RNA		1.0 (to 10.0)			
Total volume	1 rxn	20.0			

[a], for Induro, RT temperature of 50–60 °C is possible and recommended synthesis time is 10 min, but the RT step was extended to the longest time, 30 minutes, possible according to the manual. [b], betaine was only used in specified cases.

In comparison to Induro protocol in Table 12, SuperScript IV (Table 13) was used with longer incubation times to ensure highest cDNA yield. The Induro protocol was later tested with betaine in 1 M final concentration in the enzyme mix to lower primer melting temperature according to previous descriptions (Henke et al., 1997).

Table 13. RT reaction setup for SuperScript IV enzyme.

Pipetting chart			Thermal cycling for RT		
Component	Notes	Volume, µl (final concentration in the reaction)	Step	Time	Temperature (°C)
SuperScript IV 5x RT buffer	Enzyme mixture	4.0	Primer annealing	5 min	65
RT enzyme SuperScript IV (200,000 U/ml)		1.0 (10 U/µl)	Cooling on ice	≥ 1 min	
RNasin Plus Ribonuclease Inhibitor (40 U/µl), catalogue N261A (Promega)		1.0 (2.0 U/µl)	Reverse transcription[a]	45 min	57
Water		to 7.0			
dNTPs, 10 mM each, catalogue #N0447 (New England Biolabs)	Primer annealing mixture	1.0 (0.5 mM each)			
Gene-specific CVA9-gen1-R primer 10 µM, Invitrogen oligo-dT_{16} 50 µM or Fermentas oligo-dT_{18} 100 µM		0.2 (0.1 µM, gene-specific), 2.0 or 1.0 (oligo-dT final concentration 5.0 µM)	Inactivation of RT enzyme	10 min	80
Water		to 12.0			
Template RNA		1.0 (to 13.0)			
Total volume	1 rxn	20.0			

[a], SuperScript IV supports up to 50 min cDNA synthesis time and up to 60 °C temperature without significant loss of performance.

The qScript protocol (Table 14) was unique in terms of enhancer solution added when gene-specific CVA9gen1-R primer was used.

Table 14. Protocol for qScript Ultra Flex RT enzyme.

Pipetting chart	Thermal cycling for RT

Component	Notes	Volume, µl (final concentration in the reaction)	Step	Time	Temperature (°C)
qScript Ultra Flex 5x Reaction Mix	Enzyme mixture	4.0 (1x)	Primer annealing	5 min	65
			Cooling on ice	≥ 1 min	
			Reverse transcription	10 min	55
Enhancer solution 10x for gene-specific primer	Primer annealing mixture	2.0 (1x)			
Gene-specific CVA9-gen1-R primer 10 µM or qScript-oligo-dT mix 10x		1.0 (0.5 µM, gene-specific) or 2.0 (1x, oligo-dT mix)	Inactivation of RT enzyme	5 min	85
Water		to 15.0			
Template RNA		1.0 (to 16.0)			
Total volume	1 rxn	20.0			

The LunaScript protocol (Table 15) was the only one in which no separate primer annealing step was performed.

Table 15. RT protocol for LunaScript RT 5 x Master Mix Kit (Primer-free).

Pipetting chart			Thermal cycling for RT		
Component	Notes	Volume, µl (final concentration in the reaction)	Step	Time	Temperature (°C)
LunaScript RT Master Mix (Primer-free) 5 x	Full reaction mixture in a single tube, no 2-phase RT step	4.0 (1x)	Reverse transcription	10 min	55
Gene-specific CVA9gen1-R primer 10 µM or Invitrogen oligo-dT_{16} 50 µM or 100 µM oligo-dT_{18} (Fermentas)		1.0 (0.5 µM, gene-specific primer), 2.0 or 1.0 (oligo-dT, final 5 µM)	Inactivation	1 min	95
Water		to 19.0			
Template RNA		1.0 (to 20.0)			
Total volume	1 rxn	20.0			

Of all RT kits used in final experiments, LunaScript and qScript Ultra Flex kits were the only master mix formulations.

4.4 Regulatory primers and cell-based infection experiments

4.4.1 Primers and PCR products

To produce EGFP-bearing viruses in the cellular experiments, plasmid pCVA9-EGFP-6, CVA9-EGFP-6-IVT-RNA and CVA9-EGFP-6 PCR products with T7 promoter at the 5' end were transfected into transgenic T7-BSR cells that stably produce T7RNAP responsible for *in vivo* transcription (Buchholz et al., 1999). CVA9 virus RNA extracted from old cell culture samples or purified virus particles was used as a control. Different PCR products were generated with regulatory primers from the laboratory collection (Table 16) to obtain variable ends in the PCR amplicons to study the effect of the primer combinations on the efficiency of the *in vivo* transcription. Standard CVA9gen1 primers were used as controls (see section 4.2.1 Primers). The PCR products were generated by Platinum Super Fi II enzyme (see section 4.2.2 High-fidelity long PCR enzymes). The methodology involving regulatory primers was partly based on previous description in Kallio (2018).

Table 16. Regulatory primers used to produce PCR amplicons with variable ends from pCVA9-EGFP-6 plasmid clone. Legends, F, forward, R, reverse for primers.

Primer label[a]	Sequence[i]
CVA9-Griggs-FL-F[b]	5'-(TTTAAAACAGCCTGTGGGTTGTTCCC)-3'
T7-CVA9-F-Rz_active[c]	5'-TAATACGACTCACTATAGGGTGTTTTAAACTGATGAGGCCGAAAGGCCGAAAACCCGGTATCCCGGGTTC(TTTAAAACAGCCTGTGGGTTGTTCCC)-3'
T7-CVA9-F-Rz_inactive[d]	5'-TAATACGACTCACTATAGGGTGTTTTAAACTGATGAGGCCGAAAGGCCGAAAACCCGGTATCCCGGGTTG(TTTAAAACAGCCTGTGGGTTGTTCCC)-3'
TATA-T7-CVA9-F[e]	5'-TAAATATACGGATGTCGACTAATACGACTCACTATAGGG(TTTAAAACAGCCTGTGGGTTGTTCCC)-3'
TATA-OCTA-T7-CVA9-F[f]	5'-ATGCAAATCAGGTGAGTCCATGGTGGTAAATATACGGATGTCGACTAATACGACTCACTAAGGG(TTTAAAACAGCCTGTGGGTTGTTCCC)-3'
CVA9gen1-R-T7_terminator_original[g]	5'-TGCAAAAAACCCCTCAAGACCCGTTTAGAGGCCCCAAGGGGTTTTTTTTTTTTTTTTTTTTTT(CCTCCGCACCGAATGCGG)-3'
CVA9gen1-R-T7_terminator_synthetic[h]	5'-AGCAAAAAACCCCGCGAGACCCCCGAAGAGGCCCCGCGGGGTTTTTTTTTTTTTTTTTTTTTT(CCTCCGCACCGAATGCGG)-3'

[a], all mutant F primers were only paired with standard CVA9gen1-R and mutant R primers with CVA9gen1-F., [b], the Griggs-FL-F control primer does not contain a T7 promoter, so this primer is used to produce PCR products functioning as negative transfection controls. [c] and [d] are controls of each other, so are [e] and [f]. [g], [h], mutant CVA9-R primers with a separate terminator for T7RNAP-mediated *in vivo* transcription, either synthetic or naturally occurring. In relation to the scheme presented in Table 16, 7 different PCR products were finally generated on a large scale and purified, [i], note that annealing part complementary to CVA9 genome sequence is enclosed within parenthesis.

The 7 PCR products generated from pCVA9-EGFP-6 cDNA clone according to primer sets in Table 16 were purified by NucleoSpin® Gel and PCR Clean-up kit (catalogue code 740609.50, MACHEREY-NAGEL, Düren, Germany). For each product, 5 · 20 µl PCR reactions were prepared and the mixes were combined. 90 µl of the total 100 µl was purified and 10 µl of the unpurified mix was compared to 10 µl of the purified product mix on agarose gel (data not shown). After the purification process, the concentration of the PCR products was set to 100 ng/µl for downstream transfection experiments by spectrophotometry. As a control, PCR product CVA9-EGFP-6 prepared with unmodified CVA9gen1 primers (section 4.2.1) was similarly purified and verified for subsequent transfections.

4.4.2 Transfections into T7-BSR cells and detection of EGFP signal

Transfections into T7-BSR cells were performed with ScreenFect® A (catalogue S3001, ScreenFect GmbH, Eggenstein-Leopoldshafen, Germany) lipid-based transfection reagent. According to manufacturer's manual, the amount of DNA, PCR product or RNA to be transfected was set to 100 ng per well. The transfection reagent was prepared according to Table 17.

Table 17. ScreenFect A transfection protocol for 96-well plate.

Notes	Components	Volumes per one well (µl)
Nucleic acid mixture	ScreenFect A dilution buffer	7.0
	Plasmid DNA, PCR product or RNA, 100 ng or water for transfection controls	1.0
Lipid complex mixture[a]	ScreenFect A dilution buffer	7.65
	ScreenFect A reagent	0.35
Final mixture[b]	1:1 mixture of nucleic acid and lipid complex	16.0
1/6 dilution of the 16 µl final mixture[c]	80 µl standard T7-BSR medium and 16 µl final mixture	96.0

[a], incubated 20 minutes before applying to nucleic acid mixture. [b], this mixture is the final transfection complex. [c], this dilution was added to confluent cells after discarding the old medium.

The prepared transfection complexes were added to confluent T7-BSR cells obtained from the laboratory collection grown on a black 96-well plate (Perkin Elmer). The T7-BSR cells were grown in DMEM (Gibco) supplemented with 10 % heat-inactivated FBS, 1 % non-essential amino acids, 1 % Glutamax (enhanced formulation of L-glutamine), 1 x penicillin-streptomycin, and geneticin at a

constant concentration of either 200 µg/ml or 500 µg/ml on every passage. This medium is referred to as standard T7-BSR culture medium in later occurrences. The supplementary antibiotic geneticin was added to eliminate cells not producing T7RNAP through evolutionary selection. In context of the T7-BSR cells, the transgene coding T7RNAP is permanently conjugated with a gene providing the cells resistance to geneticin (Buchholz et al., 1999).

The cells were grown in standard T25 and T75 flasks at +37 °C in 5 % CO_2, and they were split by trypsin-EDTA every 3 to 5 days in a ratio ranging from 1:4 to 1:10. The transfections were performed by the 2-step method described in ScreenFect A manual. Upon splitting, 20 000 cells were added per each well of the black 96-well plate in 80 µl of standard T7-BSR medium and the cells were grown on the plate for 24 hours. On the following day, all transfections were performed for duplicate wells by the protocol in Table 17. Samples in Table 18 were used in the transfections.

Table 18. List of the different PCR products, plasmids, and RNAs used in the transfection experiments. Legends, F, forward, R, reverse for primers.

Plasmid, RNA or PCR product indicated by primers used		Description (p, plasmid clone)
1	CVA9gen1-F + CVA9gen1-R	PCR product from pCVA9-EGFP-6 clone, no regulatory elements, only T7 promoter
2	CVA9-Griggs-FL-F + CVA9gen1-R	PCR product from pCVA9-EGFP-6 clone, no T7 promoter
3	T7-CVA9-F-Rz_active + CVA9gen1-R	PCR product from pCVA9-EGFP-6 clone, includes T7 promoter
4	T7-CVA9-F-Rz_inactive + CVA9gen1-R	PCR product from pCVA9-EGFP-6 clone, includes T7 promoter
5	TATA-T7-CVA9-F + CVA9gen1-R	PCR product from pCVA9-EGFP-6 clone, includes T7 promoter
6	TATA-OCTA-T7-CVA9-F + CVA9gen1-R	PCR product from pCVA9-EGFP-6 clone, includes T7 promoter
7	CVA9gen1-R-T7_terminator_original + CVA9gen1-F	PCR product from pCVA9-EGFP-6 clone, includes T7 promoter
8	CVA9gen1-R-T7_terminator_synthetic + CVA9gen1-F	PCR product from pCVA9-EGFP-6 clone, includes T7 promoter
9	pcDNA3-GFP	Control plasmid, GFP under CMV promoter, transfection control
10	pGEM3-GFP	Control plasmid, GFP under T7 promoter, control for verifying T7RNAP production in T7-BSR cells
11	pGFP-7	Control plasmid, GFP under CMV promoter, transfection control
12	pCVA9-EGFP-6	CVA9-EGFP-6 plasmid clone

Plasmid, RNA or PCR product indicated by primers used		Description (p, plasmid clone)
13	CVA9-EGFP-6-IVT-RNA	IVT-RNA of CVA9 made from CVA9-EGFP-6 PCR product
14[a]	CVA9 pool RNA	CVA9 vRNA extracted from infectious specimen, no EGFP insert

a, 10^8 copies of CVA9 pool RNA were transfected instead of 100 ng because of the low concentration of RNA extracted from a cell culture sample. Otherwise, 100 ng of plasmid DNA, PCR product or RNA was used per well.

The transfected T7-BSR cells were incubated for 24–48 hours before fixing or freezing the plate for virus harvesting. The progression of viral infection was followed by the detection of the cytopathic effect and increasing levels of EGFP fluorescence generated by picornavirus replication and the subsequent translation of the EGFP insert in the viral clone. Fluorescent microscopy was performed via EVOS FL Auto system (Life Technologies) at magnifications of 10 x and 20 x, and the obtained images were processed with PowerPoint (Microsoft).

After 24- or 48-hours post-transfection, the T7-BSR cells were fixed at room temperature by removing the medium and washing them with 3 x 100 µl PBS per well before adding 100 µl 4 % formaldehyde in PBS per well. The cells were incubated with the 4 % formaldehyde solution for 20 minutes and then washed again with 3 x 100 µl PBS per well. The nuclei of the fixed T7-BSR cells were stained with 60 µl DAPI (1:2 000 dilution in PBS from stock 5 mg/ml) for 15 minutes in the dark after which the cells were washed with 3 x 100 µl PBS.

A549 cells from the laboratory collection were cultured in DMEM (Gibco), supplemented with 10 % inactivated FBS, 1 % Glutamax and 1 x penicillin streptomycin and incubated at +37 °C in 5 % CO_2 atmosphere. Splitting was performed by trypsin-EDTA approximately 2 x per week in ratio 1:3 to 1:5, and the cells were grown in standard T25 and T75 flasks. For secondary infection assays, 20 000 A549 cells in 100 µl medium were added to each well of a transparent 96-well plate. Frozen black T7-BSR plate stored at –80 °C was thawed and 10 µl supernatant taken from specified wells was added to confluent A549 cells in 100 µl fresh medium per well. In total, 3 columns per each virus sample were prepared on the A549 plate with 1:10 dilution from the initial column until 1:1000 dilution of the original virus-containing supernatant was reached in the 3rd column. Spread of possible secondary infection in the A549 cells was followed by light microscopy.

5 Acknowledgements

I would like to thank my supervisor Dr. Petri Susi from The Picornavirus Laboratory and all other staff at Medisiina D7 involved in this project. Their effort and technical support gave me a piece of mind during my work.

6 Abbreviations list

cDNA	Complementary DNA
CMV	Cytomegalovirus
Coxsackievirus A9	CVA9
C_q	Cycle of quantification (qPCR threshold value)
HFMD	Hand-foot-and-mouth disease
IVT	*In vitro* transcription
NTC	No template control
qPCR	Quantitative PCR
RT	Reverse transcriptase / reverse transcription
RT-qPCR	Reverse transcription quantitative PCR
Thermus aquaticus	*Taq*
T7RNAP	T7 RNA polymerase
vRNA	Virus RNA

References

Al-Hello, H., P. Ylipaasto, T. Smura, E. Rieder, T. Hovi, and M. Roivainen. 2009. Amino acids of Coxsackie B5 virus are critical for infection of the murine insulinoma cell line, MIN-6. *J Med Virol*. 81:296–304. doi:10.1002/jmv.21391.

Amadori, M., G. Volpe, P. Defilippi, and C. Berneri. 1997. Phenotypic Features of BHK-21 Cells Used for Production of Foot-and-mouth Disease Vaccine. *Biologicals*. 25:65–73. doi:10.1006/BIOL.1996.0061.

Amiri, S., S. Adibzadeh, S. Ghanbari, B. Rahmani, M.H. Kheirandish, A. Farokhi-Fard, M.S. Dastjerdeh, and F. Davami. 2023. CRISPR-interceded CHO cell line development approaches. *Biotechnol Bioeng*. 120:865–902. doi:10.1002/BIT.28329,.

Andino, R., N. Böddeker, D. Silvera, and A. V. Gamarnik. 1999. Intracellular determinants of picornavirus replication. *Trends Microbiol*. 7:76–82. doi:10.1016/S0966-842X(98)01446-2.

Andino, R., K. Kirkegaard, A. MacAdam, V.R. Racaniello, and A.B. Rosenfeld. 2023. The Picornaviridae Family: Knowledge Gaps, Animal Models, Countermeasures, and Prototype Pathogens. *Journal of Infectious Diseases*. 228:S427–S445. doi:10.1093/infdis/jiac426.

Aswathyraj, S., G. Arunkumar, E.K. Alidjinou, and D. Hober. 2016. Hand, foot and mouth disease (HFMD): emerging epidemiology and the need for a vaccine strategy. *Med Microbiol Immunol*. 205:397–407. doi:10.1007/s00430-016-0465-y.

Bandwar, R.P., Y. Jia, N.M. Stano, and S.S. Patel. 2002. Kinetic and thermodynamic basis of promoter strength: Multiple steps of transcription initiation by T7 RNA polymerase are modulated by the promoter sequence. *Biochemistry*. 41:3586–3595. doi:10.1021/bi0158472.

Bedard, K.M., and B.L. Semler. 2004. Regulation of picornavirus gene expression. *Microbes Infect*. 6:702–713. doi:10.1016/J.MICINF.2004.03.001.

Belsham, G.J. 2009. Divergent picornavirus IRES elements. *Virus Res*. 139:183–92. doi:10.1016/j.virusres.2008.07.001.

Borkotoky, S., and A. Murali. 2018. The highly efficient T7 RNA polymerase: A wonder macromolecule in biological realm. *Int J Biol Macromol*. 118:49–56. doi:10.1016/j.ijbiomac.2018.05.198.

Brisson, M., Y. He, S. Li, J.P. Yang, and L. Huang. 1999. A novel T7 RNA polymerase autogene for efficient cytoplasmic expression of target genes. *Gene Ther*. 6:263–270. doi:10.1038/sj.gt.3300827.

Buchholz, U.J., S. Finke, and K.K. Conzelmann. 1999. Generation of bovine respiratory syncytial virus (BRSV) from cDNA: BRSV NS2 is not essential for virus replication in tissue culture, and the human RSV leader region acts as a functional BRSV genome promoter. *J Virol*. 73:251–9. doi:10.1128/JVI.73.1.251-259.1999.

Bustin, S.A. 2010. Why the need for qPCR publication guidelines?—The case for MIQE. *Methods*. 50:217–226. doi:10.1016/J.YMETH.2009.12.006.

Chang, K.H., P. Auvinen, T. Hyypiä, and G. Stanway. 1989. The nucleotide sequence of coxsackievirus A9; implications for receptor binding and enterovirus classification. *J Gen Virol*. 70 (Pt 12):3269–80. doi:10.1099/0022-1317-70-12-3269.

Domingo, E., C. Escarmís, E. Lázaro, and S.C. Manrubia. 2005. Quasispecies dynamics and RNA virus extinction. *Virus Res*. 107:129–139. doi:10.1016/j.virusres.2004.11.003.

Dunn, J.J., B. Krippl, K.E. Bernstein, H. Westphal, and F. William Studier. 1988. Targeting bacteriophage T7 RNA polymerase to the mammalian cell nucleus. *Gene*. 68:259–266. doi:10.1016/0378-1119(88)90028-5.

Fu, M., J. Bai, S. Gao, Z. Chang, X. Zhou, and J.-E. Long. 2021. Construction and characterization of an infectious cDNA clone of enterovirus 71: a rapid method for rescuing infectious virus based on stable cells expressing T7 polymerase. *Arch Virol*. 166:627–632. doi:10.1007/s00705-020-04940-9.

Garmaroudi, F.S., D. Marchant, R. Hendry, H. Luo, D. Yang, X. Ye, J. Shi, and B.M. McManus. 2015. Coxsackievirus B3 Replication and Pathogenesis. *Future Microbiol*. 10:629–653. doi:10.2217/fmb.15.5.

Heikkilä, O., M. Kainulainen, and P. Susi. 2011. A combined method for rescue of modified enteroviruses by mutagenic primers, long PCR and T7 RNA polymerase-driven in vivo transcription. *J Virol Methods*. 171:129–133. doi:10.1016/j.jviromet.2010.10.013.

Heikkilä, O., P. Susi, T. Tevaluoto, H. Härmä, V. Marjomäki, T. Hyypiä, and S. Kiljunen. 2010. Internalization of Coxsackievirus A9 Is Mediated by β2-Microglobulin, Dynamin, and Arf6 but Not by Caveolin-1 or Clathrin. *J Virol*. 84:3666. doi:10.1128/JVI.01340-09.

Henke, W., K. Herdel, K. Jung, D. Schnorr, and S.A. Loening. 1997. Betaine improves the PCR amplification of GC-rich DNA sequences. *Nucleic Acids Res*. 25:3957–3958. doi:10.1093/NAR/25.19.3957,.

Huttunen, M., M. Waris, R. Kajander, T. Hyypiä, and V. Marjomäki. 2014. Coxsackievirus A9 Infects Cells via Nonacidic Multivesicular Bodies. *J Virol*. 88:5138–5151. doi:10.1128/JVI.03275-13/ASSET/D91C72C1-3627-48CB-83E2-03550E33D642/ASSETS/GRAPHIC/ZJV9990989520010.JPEG.

Hymas, W.C., W.K. Aldous, E.W. Taggart, J.B. Stevenson, and D.R. Hillyard. 2008. Description and validation of a novel real-time RT-PCR enterovirus assay. *Clin Chem*. 54:406–13. doi:10.1373/clinchem.2007.095414.

Ji, C., Y. Zhang, Y. Feng, X. Zhang, K. Wang, J. Ma, Z. Pan, and H. Yao. 2023. A polymerase mechanism-based strategy constructing attenuated clones of enterovirus for vaccine vector development. *Virology*. 580:1–7. doi:10.1016/j.virol.2023.01.007.

Kallio, T. 2018. Infektiivisen pikornaviruksen tuottaminen virus-RNA:sta. University of Turku. 1–75 pp.

Karunanathie, H., P.S. Kee, S.F. Ng, M.A. Kennedy, and E.W. Chua. 2022. PCR enhancers: Types, mechanisms, and applications in long-range PCR. *Biochimie*. 197:130–143. doi:10.1016/j.biochi.2022.02.009.

Kok, C.C., and P.C. McMinn. 2009. Picornavirus RNA-dependent RNA polymerase. *International Journal of Biochemistry and Cell Biology*. 41:498–502. doi:10.1016/j.biocel.2008.03.019.

Koskinen, M. 2023. Development of RT-PCR based method for genome amplification of human picornaviruses and rescue of viable viruses. University of Turku. 1–53 pp.

Lazouskaya, N. V., E.A. Palombo, C.-L. Poh, and P.A. Barton. 2014. Construction of an infectious cDNA clone of Enterovirus 71: Insights into the factors ensuring experimental success. *J Virol Methods*. 197:67–76. doi:10.1016/j.jviromet.2013.12.005.

Leister, D., and R. Thompson. 1996. Production of full-length cDNA from a picornaviral genome by RT-PCR. *Trends Genet*. 12:11. doi:10.1016/s0168-9525(96)90084-0.

Li, P., X. Ma, X. Bai, P. Sun, H. Yuan, Y. Cao, K. Li, H. Bao, Y. Fu, J. Zhang, Y. Chen, D. Li, Z. Li, Z. Lu, and Z. Liu. 2020. Identification of the largest non-essential regions of the C-terminal portion in 3A protein of foot-and-mouth disease virus for replication in cell culture. *Virol J*. 17:137. doi:10.1186/s12985-020-01379-x.

Lin, J.-Y., T.-C. Chen, K.-F. Weng, S.-C. Chang, L.-L. Chen, and S.-R. Shih. 2009. Viral and host proteins involved in picornavirus life cycle. *J Biomed Sci*. 16:103. doi:10.1186/1423-0127-16-103.

Lindberg, A.M., C. Polacek, and S. Johansson. 1997. Amplification and cloning of complete enterovirus genomes by long distance PCR. *J Virol Methods*. 65:191–9. doi:10.1016/s0166-0934(97)02178-2.

van der Linden, L., K.C. Wolthers, and F.J.M. van Kuppeveld. 2015. Replication and Inhibitors of Enteroviruses and Parechoviruses. *Viruses*. 7:4529–62. doi:10.3390/v7082832.

Liu, H., and H. Luo. 2021. Development of Group B Coxsackievirus as an Oncolytic Virus: Opportunities and Challenges. *Viruses*. 13. doi:10.3390/v13061082.

Lönnrot, M., M. Sjöroos, K. Salminen, M. Maaronen, T. Hyypiä, and H. Hyöty. 1999. Diagnosis of enterovirus and rhinovirus infections by RT-PCR and time-resolved fluorometry with lanthanide chelate labeled probes. *J Med Virol*. 59:378–84.

Lyu, K., G.C. Wang, Y.L. He, J.F. Han, Q. Ye, C.F. Qin, and R. Chen. 2015. Crystal structures of enterovirus 71 (EV71) recombinant virus particles provide insights into vaccine design. *Journal of Biological Chemistry*. 290:3198–3208. doi:10.1074/jbc.M114.624536.

Mairhofer, J., A. Wittwer, M. Cserjan-Puschmann, and G. Striedner. 2015. Preventing T7 RNA Polymerase Read-through Transcription—A Synthetic Termination Signal Capable of Improving Bioprocess Stability. *ACS Synth Biol*. 4:265–273. doi:10.1021/sb5000115.

McCullers, J.A. 2016. The Role of Punctuated Evolution in the Pathogenicity of Influenza Viruses. *Microbiol Spectr*. 4. doi:10.1128/microbiolspec.EI10-0001-2015.

McLeish, N.J., J. Witteveldt, L. Clasper, C. McIntyre, E.C. McWilliam Leitch, A. Hardie, S. Bennett, R. Gunson, W.F. Carman, S.A. Feeney, P. V Coyle, B. Vipond, P. Muir, K. Benschop, K. Wolthers, M. Waris, R. Osterback, I. Johannessen, K. Templeton, H. Harvala, and P. Simmonds. 2012. Development and assay of RNA transcripts of enterovirus species A to D, rhinovirus species a to C, and human

parechovirus: assessment of assay sensitivity and specificity of real-time screening and typing methods. *J Clin Microbiol*. 50:2910–7. doi:10.1128/JCM.01172-12.

Mocé-Llivina, L., F. Lucena, and J. Jofre. 2004. Double-layer plaque assay for quantification of enteroviruses. *Appl Environ Microbiol*. 70:2801–2805. doi:10.1128/AEM.70.5.2801-2805.2004,.

Nishioka, M., H. Mizuguchi, S. Fujiwara, S. Komatsubara, M. Kitabayashi, H. Uemura, M. Takagi, and T. Imanaka. 2001. Long and accurate PCR with a mixture of KOD DNA polymerase and its exonuclease deficient mutant enzyme. *J Biotechnol*. 88:141–149. doi:10.1016/S0168-1656(01)00275-9.

Österback, R., T. Tevaluoto, T. Ylinen, V. Peltola, P. Susi, T. Hyypiä, and M. Waris. 2013. Simultaneous Detection and Differentiation of Human Rhino- and Enteroviruses in Clinical Specimens by Real-Time PCR with Locked Nucleic Acid Probes. *J Clin Microbiol*. 51:3960–3967. doi:10.1128/JCM.01646-13.

De Palma, A.M., I. Vliegen, E. De Clercq, and J. Neyts. 2008. Selective inhibitors of picornavirus replication. *Med Res Rev*. 28:823–84. doi:10.1002/med.20125.

Royston, L., and C. Tapparel. 2016. Rhinoviruses and respiratory enteroviruses: Not as simple as ABC. *Viruses*. 8. doi:10.3390/v8010016.

Ruijter, J.M., C. Ramakers, W.M.H. Hoogaars, Y. Karlen, O. Bakker, M.J.B. van den Hoff, and A.F.M. Moorman. 2009. Amplification efficiency: linking baseline and bias in the analysis of quantitative PCR data. *Nucleic Acids Res*. 37:e45–e45. doi:10.1093/nar/gkp045.

Sandig, V., A. Lieber, S. Bähring, and M. Strauss. 1993. A phage T7 class-III promoter functions as a polymerase II promoter in mammalian cells. *Gene*. 131:255–259. doi:10.1016/0378-1119(93)90302-J.

Sin, J., V. Mangale, W. Thienphrapa, R.A. Gottlieb, and R. Feuer. 2015. Recent progress in understanding coxsackievirus replication, dissemination, and pathogenesis. *Virology*. 484:288–304. doi:10.1016/J.VIROL.2015.06.006.

Śpibida, M., B. Krawczyk, M. Olszewski, and J. Kur. 2017. Modified DNA polymerases for PCR troubleshooting. *J Appl Genet*. 58:133–142. doi:10.1007/S13353-016-0371-4/TABLES/3.

Steil, B.P., and D.J. Barton. 2009. Cis-active RNA elements (CREs) and picornavirus RNA replication. *Virus Res*. 139:240–252. doi:10.1016/J.VIRUSRES.2008.07.027.

Terpe, K. 2013. Overview of thermostable DNA polymerases for classical PCR applications: From molecular and biochemical fundamentals to commercial systems. *Appl Microbiol Biotechnol*. 97:10243–10254. doi:10.1007/S00253-013-5290-2/TABLES/3.

Vázquez-Calvo, Á., J.C. Saiz, K.C. McCullough, F. Sobrino, and M.A. Martín-Acebes. 2012. Acid-dependent viral entry. *Virus Res*. 167:125–137. doi:10.1016/J.VIRUSRES.2012.05.024.

Vilen, H., J.-M. Aalto, A. Kassinen, L. Paulin, and H. Savilahti. 2003. A direct transposon insertion tool for modification and functional analysis of viral genomes. *J Virol*. 77:123–34. doi:10.1128/jvi.77.1.123-134.2003.

Xu, L.L., C. Shan, C.L. Deng, X.D. Li, B. Di Shang, H.Q. Ye, S.Q. Liu, Z.M. Yuan, Q.Y. Wang, P.Y. Shi, and B. Zhang. 2015. Development of a stable Gaussia luciferase enterovirus 71 reporter virus. *J Virol Methods*. 219:62–66. doi:10.1016/j.jviromet.2015.03.020.

Yan, J., M. Wang, X. Li, J. Fan, R. Yu, M. Kang, Y. Zhang, J. Xu, X. Zhang, and S. Zhang. 2024. Construction of an infectious clone for enterovirus A89 and mutagenesis analysis of viral infection and cell binding. *Microbiol Spectr*. 12. doi:10.1128/spectrum.03332-23.

Yeong, M.Y., P.S. Cheow, S. Abdullah, A.A.L. Song, J. Lei-Rossmann, T.K. Tan, K. Yusoff, and S.L. Chia. 2021. Development of a T7 RNA polymerase expressing cell line using lentivirus vectors for the recovery of recombinant Newcastle disease virus. *J Virol Methods*. 291:114099. doi:10.1016/J.JVIROMET.2021.114099.

Yu, R., M. Wang, L. Liu, J. Yan, J. Fan, X. Li, M. Kang, J. Xu, X. Zhang, and S. Zhang. 2023. The development and characterization of a stable Coxsackievirus A16 infectious clone with Nanoluc reporter gene. *Front Microbiol*. 13. doi:10.3389/fmicb.2022.1101850.

Zell, R. 2018. Picornaviridae-the ever-growing virus family. *Arch Virol*. 163:299–317. doi:10.1007/s00705-017-3614-8.

Zell, R., N.J. Knowles, and P. Simmonds. 2021. A proposed division of the family Picornaviridae into subfamilies based on phylogenetic relationships and functional genomic organization. *Arch Virol*. 166:2927–2935. doi:10.1007/s00705-021-05178-9.

Zhang, X., M. Paget, C. Wang, Z. Zhu, and H. Zheng. 2020. Innate immune evasion by picornaviruses. *Eur J Immunol*. 50:1268–1282. doi:10.1002/eji.202048785.

Zheng, H., H. Tian, Y. Jin, J. Wu, Y. Shang, S. Yin, X. Liu, and Q.G. Xie. 2009. Development of a hamster kidney cell line expressing stably T7 RNA polymerase using retroviral gene transfer technology for efficient rescue of infectious foot-and-mouth disease virus. *J Virol Methods*. 156:129–137. doi:10.1016/J.JVIROMET.2008.11.010.

Zhu, P., W. Ji, D. Li, Z. Li, Y. Chen, B. Dai, S. Han, S. Chen, Y. Jin, and G. Duan. 2023. Current status of hand-foot-and-mouth disease. *J Biomed Sci*. 30:15. doi:10.1186/s12929-023-00908-4.